

Thymic negative selection is functional in NOD mice

Michael Mingueneau, Wenyu Jiang, Markus Feuerer, Diane Mathis, and Christophe Benoist

Division of Immunology, Department of Microbiology and Immunobiology, Harvard Medical School, Boston, MA 02115

Based on analyses of multiple TCR transgenic (tg) models, the emergence of pathogenic T cells in diabetes-prone NOD mice has been ascribed to a failure to censure autoreactive clones in the thymus. In contrast, using isolated and preselected thymocytes, we show that nonobese diabetic (NOD) genetic variation impairs neither clonal deletion nor downstream transcriptional programs. However, we find that NOD genetic variation influences $\alpha\beta/\gamma\delta$ -lineage decisions promoted by early expression of tg $\alpha\beta$ -TCRs at the double-negative (DN) stage. In B6 and other genetic backgrounds, tg $\alpha\beta$ -TCRs behave like $\gamma\delta$ -TCRs and commit a large fraction of DNs toward the $\gamma\delta$ -lineage, thereby decreasing the size of the double-positive (DP) pool, which is efficiently positively and negatively selected. In NOD DNs, $\alpha\beta$ -TCR signalosomes instead behave like pre-TCRs, resulting in high numbers of DPs competing for limited selection niches, and poor positive and negative selection. Once niche effects are neutralized in mixed bone marrow chimeras, positive and negative selection are equally efficient on B6 and NOD backgrounds. Biochemical analysis revealed a selective defect in the activation of Erk1/2 downstream of NOD $\alpha\beta$ -TCR signalosomes. Therefore, NOD genetic variation influences $\alpha\beta/\gamma\delta$ -lineage decisions when the $\alpha\beta$ -TCR heterodimer is prematurely expressed, but not the process of negative selection.

CORRESPONDENCE

Diane Mathis and
Christophe Benoist:
cbdm@hms.harvard.edu

Abbreviations used: DN, double negative; DP, double positive; FTOC, fetal thymic organ culture; NOD, nonobese diabetic; SP, single positive; T1D, type-1 diabetes; T conv cell, conventional T cell; tg, transgenic; T reg cell, regulatory T cell.

Two major mechanisms contribute to the establishment of a self-restricted but mostly non-autoreactive T cell repertoire (Starr et al., 2003). First, after the onset of $\alpha\beta$ -TCR expression in CD4⁺CD8⁺ (double positive [DP]) thymocytes, positive selection rescues from programmed cell death those cells expressing TCRs that recognize with sufficient (but low) affinity self-peptides complexed to MHC molecules. As the second arm of central tolerance, negative selection—mainly through clonal deletion—eliminates from the repertoire T cells that are equipped with TCRs of higher affinities (Siggs et al., 2006), although a small subset of cells expressing self-reactive TCRs is rescued and diverted toward regulatory lineages such as regulatory T cells (T reg cells; Baldwin et al., 2004).

Mechanistically, the opposite biological outcomes—survival and cell death—promoted by the same $\alpha\beta$ -TCR in conditions of positive and negative selection are driven by temporally, spatially, quantitatively, and qualitatively distinct signals. One of the most differential pathways is the RasGRP1-driven activation of Erk1/2 MAP

kinases (Teixeiro and Daniels, 2010), which plays an obligatory role during positive selection but is dispensable for negative selection (McGargill et al., 2009). Conversely, Grb2-SOS-driven activation of p38 and JNK MAP kinases is required for negative but not positive selection (Siggs et al., 2006). A few other molecules are known to participate in negative selection, including Erk5, Bim, Nur77, and Mink (Sohn et al., 2007).

Although there is ample evidence for the importance of dominant tolerance and T reg cells for preventing autoimmunity, data supporting an equivalent role for deletional tolerance are less abundant. Some evidence has come from the autoimmune disease caused by the disruption of the *Aire* gene (Mathis and Benoist, 2009), and a role for central tolerance defects in the pathogenesis of type-1 diabetes (T1D) has also been proposed, based on several observations. First, genetically controlled variation in the level of insulin gene expression in the human thymus has been linked to susceptibility to T1D, and proposed to reflect

Markus Feuerer's present address is Immune Tolerance Group, German Cancer Research Center (DKFZ), Heidelberg 69120, Germany.

© 2012 Mingueneau et al. This article is distributed under the terms of an Attribution-Noncommercial-Share Alike-No Mirror Sites license for the first six months after the publication date (see <http://www.rupress.org/terms>). After six months it is available under a Creative Commons License (Attribution-Noncommercial-Share Alike 3.0 Unported license, as described at <http://creativecommons.org/licenses/by-nc-sa/3.0/>).

a variable degree of tolerance induction (Pugliese et al., 1997). Second, nonobese diabetic (NOD) thymocytes are resistant to anti-CD3–provoked clonal deletion, although this point has been debated (Kishimoto and Sprent, 2001; Villunger et al., 2003). Several TCR transgenic (tg) derivatives of the NOD mouse model of T1D have been used to address this issue. In particular, studies using the diabetogenic BDC2.5 and AI4 TCRs that recognize natural autoantigens in the pancreas (Choisy-Rossi et al., 2004; Zucchelli et al., 2005; Holler et al., 2007; Serreze et al., 2008) or the 3A9 TCR specific for a transgene–encoded pancreatic neo–antigen (Lesage et al., 2002; Liston et al., 2004, 2007) have shown that autoreactive clones appear not to be purged efficiently in NOD mice. Several of the faulty molecular candidates were found to be common to all three TCR tg models, including *Bim* and *Nur77* genes. A body of literature, not easily integrated, indicates that these defects may result from proximal and multifocal signaling defects downstream from the TCR in NOD mice (Rapoport et al., 1993, 1999; Salojin et al., 1997; Zhang et al., 1998).

A challenge remains to understand how signaling and transcriptional defects downstream of $\alpha\beta$ -TCRs on the NOD background lead to selective functional outcomes, and how these are affected by NOD genetic variation. In the models used previously by ourselves and others, careful dissection was potentially confounded by effects of NOD genetic variation at multiple stages of thymocyte differentiation. Here, by using experimental systems in which this parameter was rigorously controlled, we arrived at a different conclusion: the phenomena interpreted as resistance to clonal deletion on the NOD background result instead from increased competition for selection niches, itself a consequence of a differential ability of NOD cells to proceed into $\alpha\beta$ over $\gamma\delta$ commitment in response to $\alpha\beta$ -TCR expression at the immature double-negative (DN) stage. This early divergence in TCR tg models reveals an unanticipated impact of NOD genetic variation on a crucial node in $\alpha\beta$ -TCR signaling networks, *Erk1/2*.

RESULTS

Clonal deletion and associated transcriptional programs are functional in NOD mice

Our earlier results (Zucchelli et al., 2005; Holler et al., 2007) showed that, as with other TCR tg systems (Lesage et al., 2002; Liston et al., 2004; Choisy-Rossi et al., 2004; Serreze et al., 2008), expression of the BDC2.5 TCR led to a dearth of DPs and small thymi on the B6^{g7} but not on the NOD background, observations which were interpreted as a differential resistance to clonal deletion. Thymocyte differentiation is a dynamic process involving several TCR–dependent checkpoints on which genetic variations can impinge. We reasoned that monoclonal and synchronized DP thymocytes, stimulated in vitro with their cognate ligand, would allow us to identify how genetic variation has an impact on the TCR signaling axis of DP thymocytes while strictly controlling other variables (in particular, potential effects of NOD genetic variation at other stages of thymocyte differentiation). Thus, we bred the BDC2.5 TCR transgene onto the B6.Rag^{−/−} and NOD.

H2^b.Rag^{−/−} backgrounds, both expressing the nonselecting A^b MHC molecule. As anticipated, the resulting mice did not harbor mature T cells and thymocyte differentiation was arrested at a preselection DP stage (Fig. S1, A and B).

Purified DP thymocytes from these mice were stimulated in vitro with mimotope–pulsed splenic APCs, and early consequences on the transcriptome were analyzed by gene expression profiling. A robust stimulation was observed after 7 h. Contrary to anticipated results, however, the responses were very similar on the NOD.H2^b and B6 backgrounds, with most of the responsive genes aligning on the diagonal of the fold change/fold change plot (Fig. 1 A), including at shorter time points and with suboptimal peptide concentrations (Fig. S1 C). This finding applied not only to T cell activation genes (Fig. 1 B) but also to negative selection–associated (*Nr4a1*, *Bcl2l11*, *Gadd45b*, and *Pdd1*) and prosurvival (*Rorc*, *Hivep2*, *Bcl2l1*, and *Bcl2*) genes (Fig. 1 C), many of which were previously found to be improperly regulated during negative selection in NOD mice (Choisy-Rossi et al., 2004; Liston et al., 2004, 2007; Zucchelli et al., 2005).

We also asked whether varying the unit affinity of the ligand might reveal a difference, using mimotope variants with different agonist potencies (Fig. 1 D). CD69 up-regulation, TCR down-modulation, and ligand-induced cell death were as efficient in NOD.H2^b as in B6 thymocytes, through a range of mimotope doses and potencies. In conclusion, preselected DP thymocytes on the NOD background showed largely unaltered TCR–dependent transcriptional and apoptotic responses.

Positive selection of class I– and class II–restricted tg TCRs is impaired in NOD mice

These results disagree with earlier conclusions made by ourselves and others, reporting central tolerance defects in NOD thymi in vivo or in fetal thymic organ cultures (FTOCs; Lesage et al., 2002; Choisy-Rossi et al., 2004; Liston et al., 2004; Zucchelli et al., 2005). In these systems, the NOD background was shown to impede the deletion of autoreactive DP and/or CD4 single-positive (SP) thymocytes, resulting in accumulation of the corresponding populations. Because whole thymi, rather than isolated cell populations, were exposed to negatively selecting ligands in these studies, compound effects of NOD alleles at several stages of thymocyte differentiation might have confounded the results. We thus decided to revisit the impact of NOD genetic variation on thymocyte selection, using adult BDC2.5 TCR tg mice on selecting NOD or B6^{g7} backgrounds.

Similar to what was observed at the fetal stage (Zucchelli et al., 2005), thymi from adult Rag-sufficient and –deficient BDC2.5/B6^{g7} mice showed a markedly reduced proportion of DPs, a much higher proportion of DN_s, more CD4SP_s, and lower total cellularity (Fig. 2, A and B) relative to BDC2.5/NOD thymi, whose overall appearance and cellularity were comparable with those of a non-tg thymus. This dearth of DPs relative to SP_s and DN_s could be interpreted as reflecting various degrees of negative selection, yet they were also compatible with a difference in efficacy of positive selection and of the DP to SP transition. Indeed, the following careful analysis of these thymi supported a defect in positive selection in BDC2.5/NOD mice:

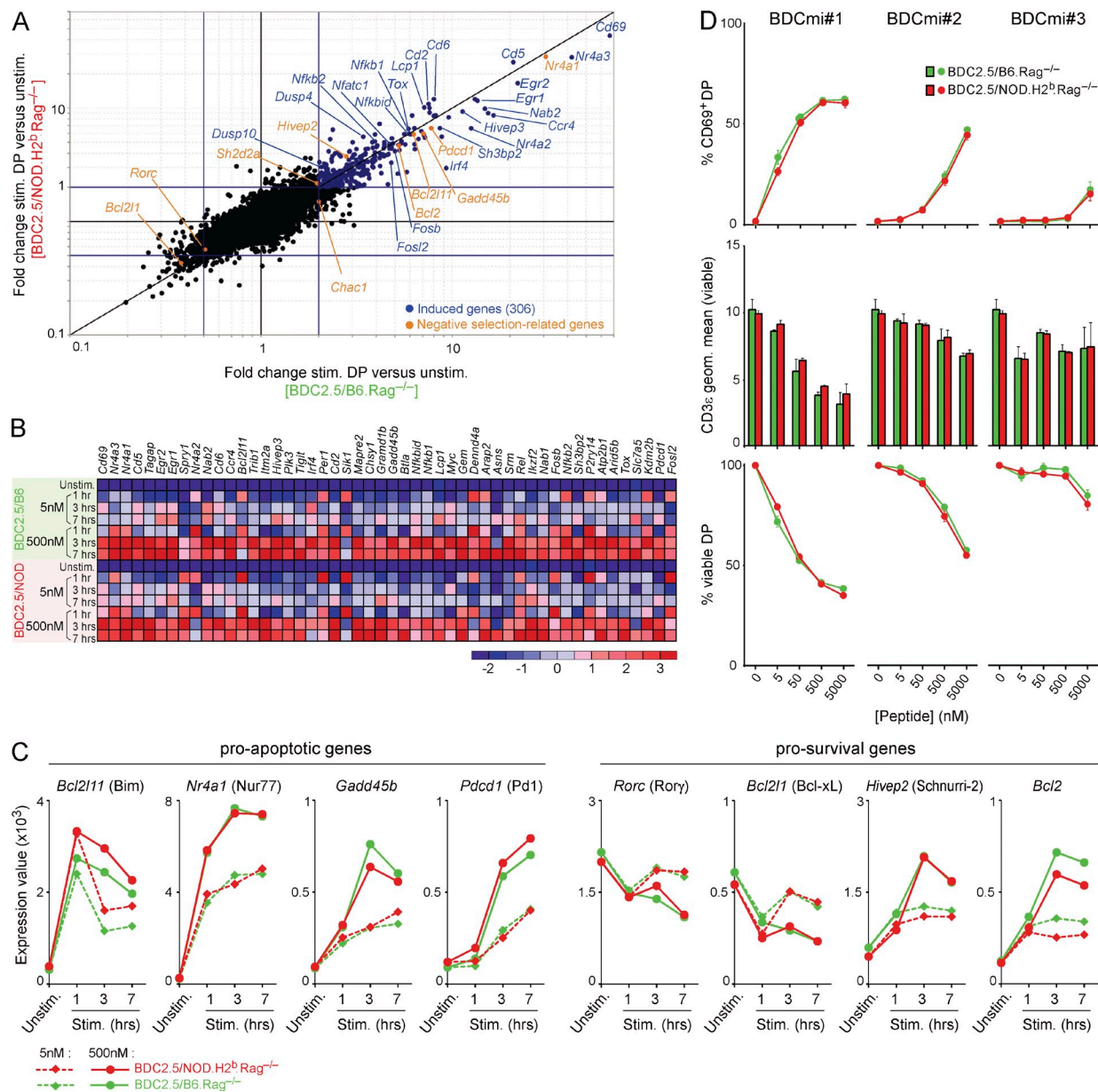


Figure 1. Negative selection is functional in NOD mice. DP thymocytes purified from mice expressing the BDC2.5 tg TCR on *Rag1*-deficient, nonselecting B6 or NOD.H2^b backgrounds, were co-cultured with mimotope-pulsed splenic APCs. DP thymocytes were analyzed by transcriptome profiling (A–C) or flow cytometry (D). (A) Fold change/fold change plot showing transcriptome changes induced by a 7-h stimulation with 500 nM BDC mimotope peptide, as the stimulated (stim.) / unstimulated (unstim.) ratio of expression in B6 (x axis) and NOD (y axis) DP thymocytes. For the unstimulated condition, DP thymocytes were incubated with unpulsed splenic cells. (B) Heat map of the 50 transcripts most induced in DPs by mimotope stimulation, in the same conditions as in A. Relative expression is color coded for two peptide concentrations and three time points (left margin). For the unstimulated (unstim.) condition, DP thymocytes were incubated with unpulsed splenic cells for 3 h. (C) Microarray expression values for selected proapoptotic and prosurvival genes in unstimulated or stimulated cells as in A, plotted versus time. (D) Stimulation by three mimotope variants (BDCmi#1–3) of different potency. Frequency of CD69⁺ cells among DP thymocytes (top), geometric mean of CD3ε expression (middle), and ligand-induced apoptosis, measured as the frequency of viable DPs (bottom), after a 20-h stimulation. Error bars indicate standard deviation of the mean. Data are means of two (A–C; $n = 2$ per genotype for $t = 1$ and 3 h and $n = 4$ per genotype for $t = 7$ h) and representative of three (D; $n \geq 2$ per genotype per experiment) independent experiments.

(A) The frequency of CD4SP thymocytes and peripheral T cells with a lower expression of the BDC2.5 clonotypic TCR (BDC^{low} population) was three to four times higher on the NOD background (Fig. 2, C and D). This resulted from increased rearrangement of endogenous genes encoding Vα chains and

surface expression of two TCR-α chains on the cell surface because BDC^{low} CD4⁺ cells were absent in *Rag*-deficient BDC2.5 mice (Fig. S2). Endogenous rearrangements of the *Tcrα* locus were reported to be promoted in TCR tg models by defects in positive selection, rather than negative selection (Buch et al., 2002).

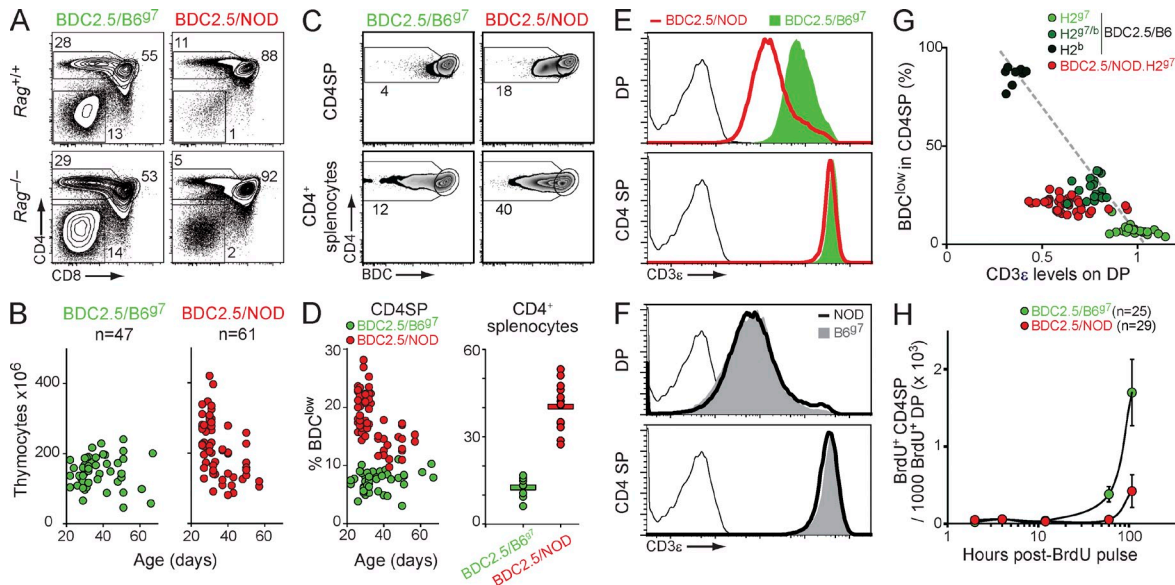


Figure 2. Impaired positive selection of BDC^{2.5} thymocytes in NOD mice. Thymocytes were isolated from polyclonal or BDC2.5 TCR tg mice on B6^{g7} or NOD backgrounds. (A) Distribution of thymocyte subsets. (B) Number of total thymocytes, versus the age of each mouse. (C) Expression of the BDC2.5 TCR, detected with the anti-clonotypic BDC antibody (Kanagawa et al., 2002), on CD4SP thymocytes (top) and CD4⁺ splenocytes (bottom). (D) Quantification of data shown in C. Horizontal lines indicate the mean. (E and F) Expression of CD3 ϵ on DP and CD4SP thymocytes from BDC2.5 TCR tg (E) and polyclonal mice (F). Thin lines indicate negative control staining. (G) Percentage of BDC^{low} CD4SP thymocytes plotted versus the geometric mean of CD3 ϵ surface expression on DP thymocytes from mice of indicated genotypes. (H) BrdU pulse-labeling experiment. Number of BrdU⁺ CD4SP per 1000 BrdU⁺ DP thymocytes over time, after a single BrdU injection. Error bars indicate standard deviation of the mean. Data are from 15 (A–G; $n \geq 40$ per genotype) and means of 8 (H; $n \geq 25$ per genotype) independent experiments.

(B) DP thymocytes from BDC2.5/NOD mice expressed 40–50% less CD3 than did their B6^{g7} counterparts (Fig. 2 E). This difference was absent in polyclonal mice (Fig. 2 F) and, thus, did not reflect a general defect in TCR expression. TCR levels on DP thymocytes from TCR tg models positively correlate with the efficiency of positive selection (Sato et al., 1996), a regulation which applied to the BDC2.5 mouse model because the gradual decrease of the availability of selecting A^{g7} molecules led to a commensurate decrease of TCR levels on

the B6 background (Fig. 2 G). On this plot, BDC2.5/NOD DPs were roughly analogous to those inefficiently selected on the hybrid BDC2.5/B6^{g7/b} background.

(C) We directly evaluated the efficacy of positive selection by performing BrdU pulse-labeling experiments. This tracer is incorporated by cycling DN and early DP thymocytes and only appears in CD4SPs a few days later, with their rate of appearance reflecting the efficacy of positive selection. Equivalent proportions of thymocytes were labeled during the pulse period (Fig. S3), but the emergence of BrdU⁺ CD4SPs was clearly faster and more effective in BDC2.5/B6^{g7} than in BDC2.5/NOD mice (Fig. 2 H and Fig. S3).

The analysis of two additional TCR tg lines (OTII and OTI; Fig. 3), as well as previous publications describing other TCR tg lines on the NOD background (3A9 and AI4; Lesage et al., 2002; Choisy-Rossi et al., 2004; Liston et al., 2007; Serreze et al., 2008), revealed that these observations were neither peculiar to the BDC2.5 model nor limited to MHCII-restricted TCR

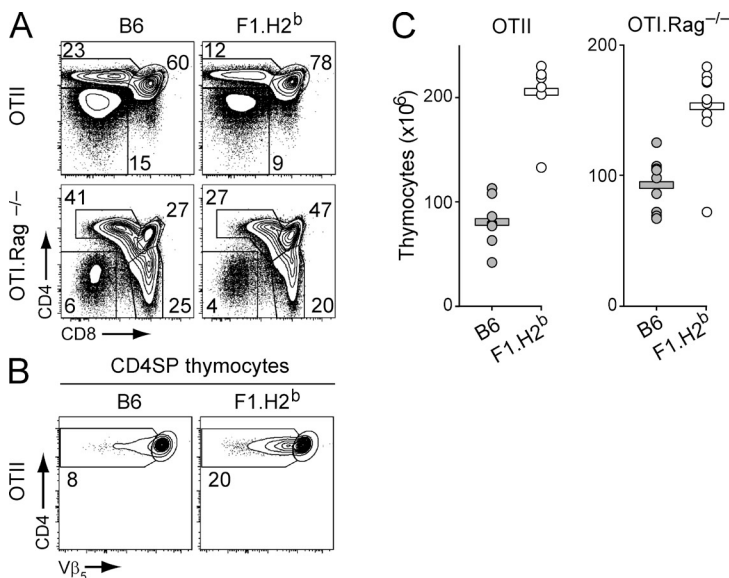


Figure 3. Impaired positive selection of MHC-II and MHC-I restricted TCRs on the NOD background. Thymocytes were isolated from mice expressing the OTII or the OTI tg TCRs on B6 or (B6xNOD.H2^b) F1 background (F1.H2^b). Shown are the distribution of thymocyte subsets (A), expression of CD4 and V β_5 tg TCR chain on CD4SP thymocytes from OTII mice (B), and number of total thymocytes (C). Horizontal lines indicate the mean. Data are representative of two independent experiments ($n \geq 3$ per genotype per experiment).

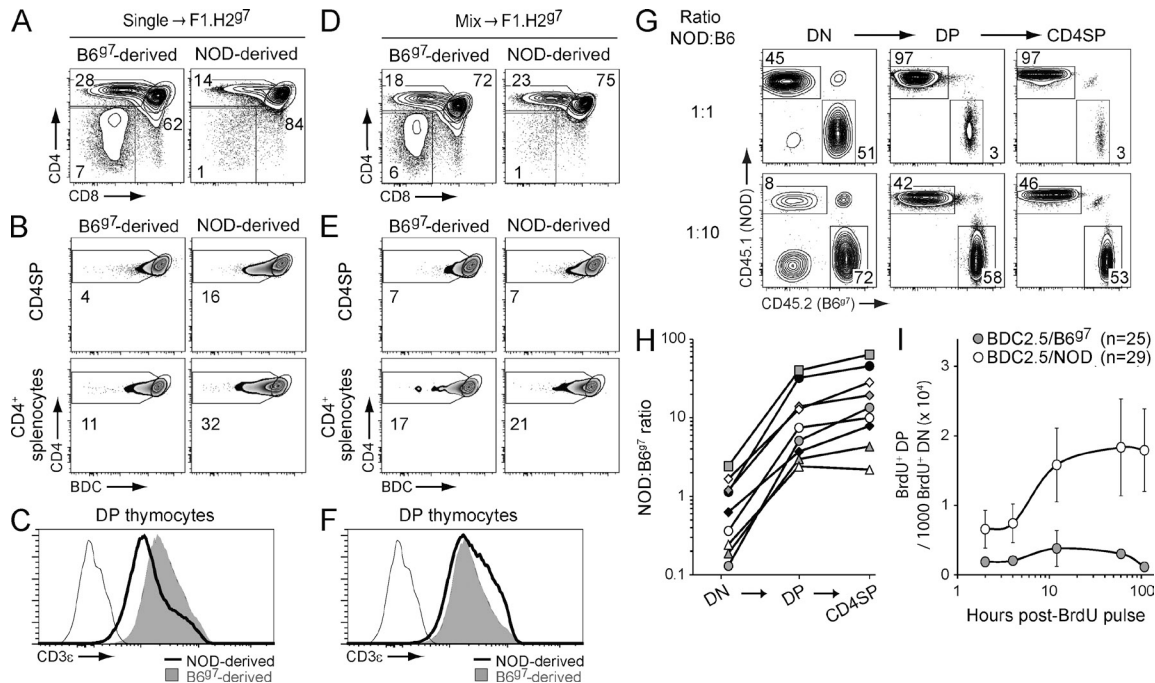


Figure 4. Higher DN to DP transition and saturation of selection niches in BDC2.5/NOD mice. Single and mixed BM chimera experiments in (B6^{g7} × NOD) F1 hosts (F1.H297; A–H) and BrdU pulse-labeling experiment in BDC2.5 TCR tg mice on B6^{g7} or NOD background (I). (A–F) Thymocytes were analyzed in F1 hosts, 8 wk after reconstitution with single (A–C) or mixed (D–F) BM cells isolated from BDC2.5 mice on B6 or NOD backgrounds. Shown are the distribution of thymocyte subsets (A and D), expression of the clonotypic BDC2.5 TCR on CD4SP thymocytes and CD4⁺ splenocytes (B and E), and of CD3ε on DP thymocytes (C and F, thin lines indicate control staining). Mean thymic cellularities of single BM chimera: 53 ± 15 , $n = 8$ (BDC2.5/B6^{g7} in F1.H297); 111 ± 31 , $n = 8$ (BDC2.5/NOD in F1.H297). (G) Expression of CD45.1 (NOD) and CD45.2 (B6^{g7}) on DN, DP, and CD4SP thymocytes from F1 mixed chimeras. The ratios of BDC2.5/NOD:BDC2.5/B6 donors are 1:1 (top) and 1:10 (bottom). (H) NOD/B6 ratios in thymic subsets of mixed chimeras, over a range of BDC2.5/NOD:BDC2.5/B6 donor ratios. Each line represents one individual chimeric mouse. (I) More efficient DN to DP transition in BDC2.5/NOD mice in noncompetitive settings. Number of BrdU⁺ DP thymocytes generated per 1,000 BrdU⁺ DN at indicated time points after a single BrdU injection. Error bars indicate standard deviation of the mean. Data are representative of two (A–C; $n = 8$ per type of chimera) and nine (D–H; $n = 38$ mixed chimera) and means of eight (I; $n \geq 25$ per genotype) independent experiments.

tg models. To avoid backcrossing steps, we took advantage of the fact that the phenotypes observed in BDC2.5/NOD mice were dominant in BDC2.5/F1(B6^{g7} × NOD) mice (unpublished data) and compared OTII and OTI TCR tg mice on B6 versus (B6 × NOD.H2^b).F1 backgrounds. F1 mice expressing the tg OTII and OTI TCRs, as well as NOD mice expressing the 3A9 (in absence of the transgene-encoded HEL TCR ligand) and AI4 tg TCRs, displayed marks of impaired positive selection similar to those seen in BDC2.5/NOD mice, including decreased SP/DP ratios (Fig. 3 A; Lesage et al., 2002, Fig. 6 a; Serreze et al., 2008, Fig. 3 A), higher frequencies of T cells expressing endogenous TCR genes (Fig. 3 B; Lesage et al., 2002, Fig. 3 c; Choisy-Rossi et al., 2004, Fig. 6 A), decreased TCR levels on DP thymocytes (Liston et al., 2007, Fig. 5 a; Serreze et al., 2008, Fig. 4), and higher total thymic cellularities (Fig. 3 C; Lesage et al., 2002, Fig. 6 c; Choisy-Rossi et al., 2004, Fig. 1 B).

Greater DN to DP transition and saturation of positive selection niches in BDC2.5/NOD mice

These several observations indicated that variation in the efficacy of positive selection was responsible for some of the phenotypic differences shown in Fig. 2 A. Positive selection is a saturable phenomenon whose efficiency is dependent on the availability

of TCR-specific selection niches (Huesmann et al., 1991). To determine whether T cell-intrinsic and/or niche effects were responsible, we set up single and mixed BM chimera experiments. When chimeras were generated by parallel transfer of BDC2.5/B6^{g7} and BDC2.5/NOD BM into F1 hosts, chimeras reproduced the differences in thymic CD4/CD8 profiles, frequencies of BDC^{low} CD4SP cells, and CD3 levels on DPs, which were previously seen in parental tg thymi (Fig. 4, A–C).

In contrast, when BDC2.5/B6^{g7} and BDC2.5/NOD T cells matured together in the same thymic environment of mixed BM chimeras, and thus faced the same competition for positive selection niches, these differences were neutralized (Fig. 4, D–F). The proportion of DPs was restored to normal in BDC2.5/B6^{g7}-derived cells, and BDC2.5/NOD-derived cells matured effectively into CD4SPs, if anything with slightly higher efficiency. Accordingly, the frequency of BDC^{low} cells and TCR levels on DP thymocytes were also normalized in mixed chimeras (Fig. 4, E and F), therefore establishing that the positive selection defect in BDC2.5/NOD mice was driven by a decreased availability of positive selection niches.

A second observation, which largely explains the difference in intraclonal competition between the parental tg strains, was made in these mixed BM chimera; we noticed that the

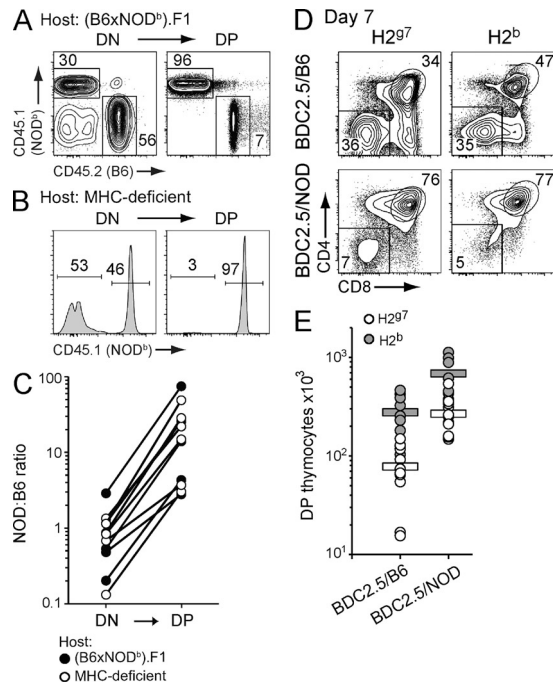


Figure 5. The greater DN to DP transition in adult and fetal thymi from BDC2.5/NOD mice is MHC independent. (A–C) Thymocytes were analyzed in indicated chimeras, 8 wk after reconstitution with mixed BM cells isolated from BDC2.5 mice on B6 and NOD.H2^b backgrounds. Expression of CD45.1 (NOD) and CD45.2 (B6) on DN and DP thymocytes, for a ratio of BDC2.5/NOD:BDC2.5/B6 donors of 1:1 (A and B) and NOD/B6 ratios in DN and DP subsets, over a range of BDC2.5/NOD:BDC2.5/B6 donor ratios (C). (D–E) BDC2.5 tg FTOCs expressing H2⁹⁷ or nonselecting H2^b MHC haplotypes were analyzed after 7 d of culture. Shown are the expression of CD4 and CD8 (D) and number of DP thymocytes in FTOCs of indicated genotypes (E). Horizontal lines indicate the mean. Data are representative of three (A–C; $n \geq 5$ per type of chimera) and two (D–E; $n \geq 8$ per genotype) independent experiments.

relative proportion of thymocytes derived from BDC2.5/NOD and BDC2.5/B6^{g7} in the reconstituted thymic subsets was very different. At a 1:1 ratio of BM cells, chimeras showed the expected 1:1 ratio in the thymic DN population (Fig. 4 G, top). However, the representation of BDC2.5/B6^{g7} progeny was greatly reduced in the DP compartment, accounting for <5% of the whole population. As a result, CD4SP and peripheral T cell compartments were largely dominated by BDC2.5/NOD-derived cells and 10:1 ratios were required in the BM inoculum to get a balanced representation of BDC2.5/B6^{g7} and BDC2.5/NOD cells at the DP stage (Fig. 4 G, bottom). On average, for various input ratios, the DN to DP transition was 10–20× more efficient on the NOD background (Fig. 4 H). BrdU pulse-labeling experiments showed that these results held true in noncompetitive settings, since much higher ratios of BrdU⁺ DP versus BrdU⁺ DN cells were observed in BDC2.5/NOD thymi than in B6^{g7} counterparts (Fig. 4 I). In hindsight, these results explained the greater number of DP thymocytes observed in adult (Fig. 2 B and Fig. 3 C; Lesage et al., 2002, Fig. 6 c;

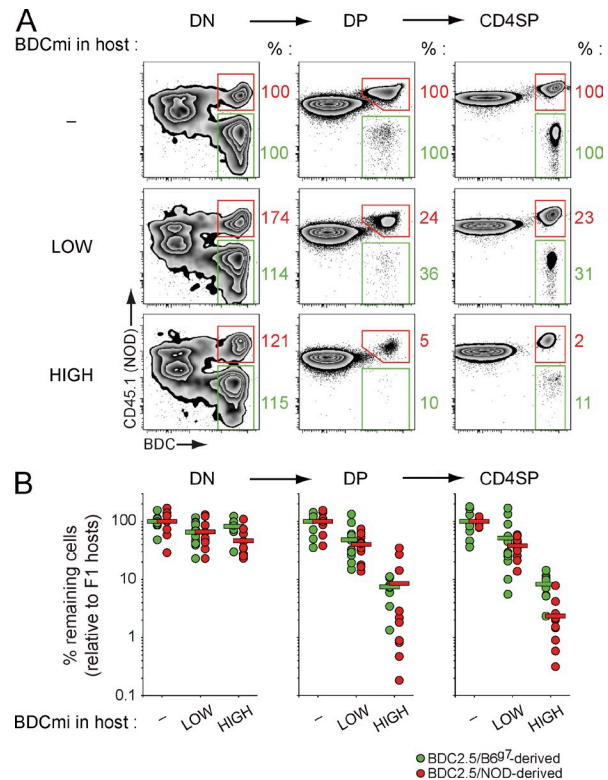


Figure 6. In vivo thymic negative selection is functional in NOD mice. Mixed BM chimera experiments in (B6⁹⁷xNOD)F1 hosts (BDCmi⁻) or F1 hosts expressing a BDC mimotope at low (BDCmi^{LOW}) or high (BDCmi^{HIGH}) levels in thymic epithelial cells. (A) Thymocytes were analyzed in indicated chimeras, 8 wk after reconstitution with mixed BM cells isolated from BDC2.5/B6⁹⁷, BDC2.5/NOD, and polyclonal F1 mice (ratio 4:1:0.3, respectively). Expression of CD45.1 (NOD) and the clonotypic BDC2.5 TCR on thymic subsets. Numbers indicate the percentage of remaining BDC2.5/B6 (green) and BDC2.5/NOD cells (red) relative to the number of cells observed in BDCmi⁻ hosts. (B) Quantification of data shown in A. Percentage of remaining thymocytes relative to the number of cells observed in BDCmi⁻ hosts. Each dot represents one individual chimeric mouse. Horizontal lines indicate the mean. Data are representative of three independent experiments ($n \geq 8$ per type of chimera).

Choisy-Rossi et al., 2004, Fig. 1 B) and fetal (Zucchelli et al., 2005) TCR tg thymi on the NOD background.

This increased DN to DP transition in BDC2.5/NOD mice was not dependent on cognate MHC recognition, and thus not a consequence of differential negative selection, as BDC2.5/NOD.H2^b-derived thymocytes also over-competed BDC2.5/B6 counterparts at the DN to DP transition in mixed chimera settings in (B6xNOD.H2^b).F1 hosts expressing the nonselecting H2^b MHC haplotype (Fig. 5, A and C), as well as in MHC-deficient hosts (Fig. 5, B and C). Symmetrically, at the fetal stage, the differential representation of DP thymocytes that was seen in BDC2.5/B6^{g7} and BDC2.5/NOD FTOCs (Zucchelli et al., 2005) was also observed on the nonselecting H2^b MHC (Fig. 5, D and E), therefore excluding any contribution of negative selection in this setting as well.

In conclusion, these results pointed to the following scenario: a thymocyte-autonomous variation primarily affected the

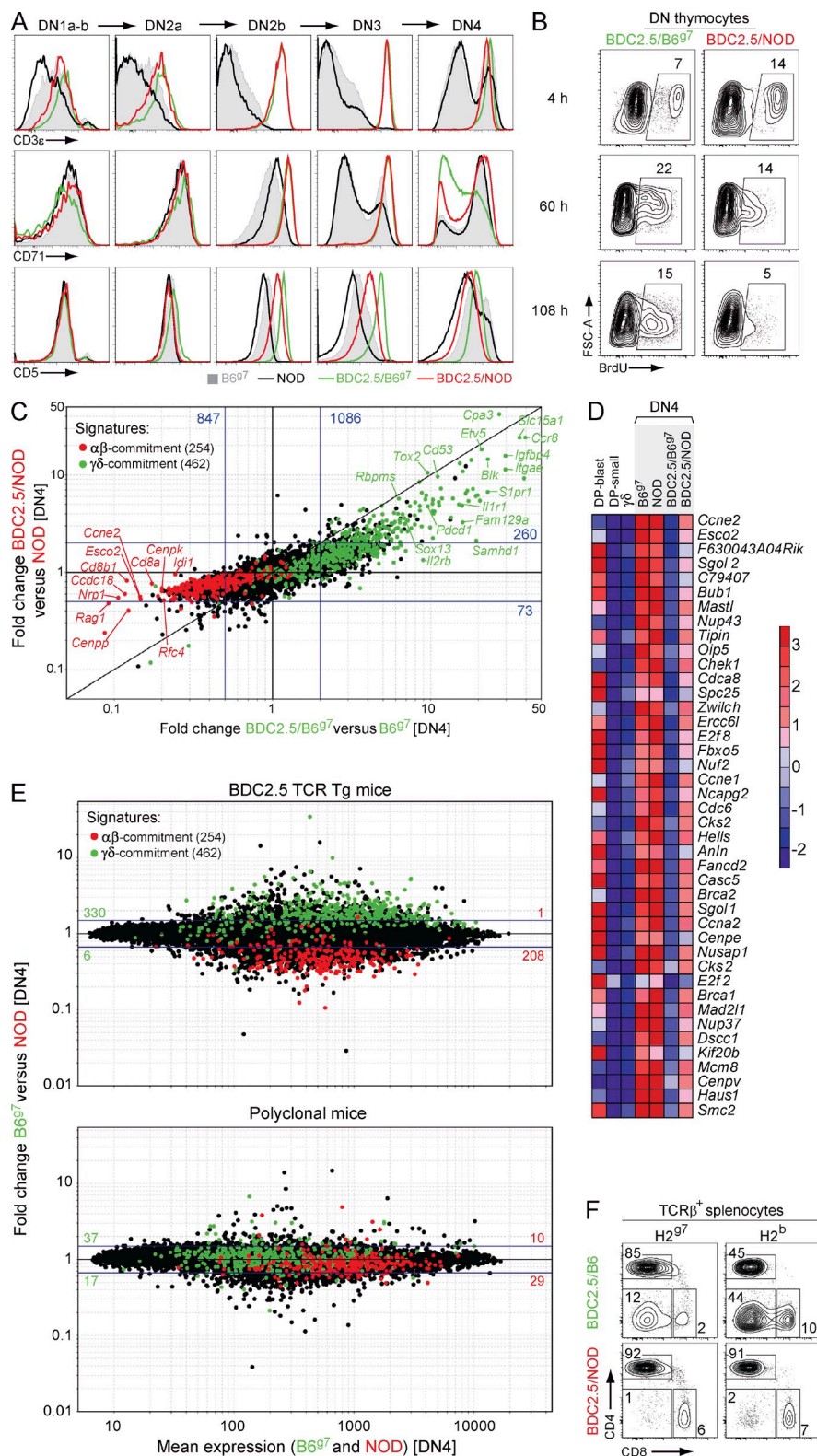


Figure 7. B6 and NOD αβ-TCRs promote opposite γδ- and αβ-lineage fates.

DN thymocytes (A–E) or splenocytes (F) were isolated from non-tg or BDC2.5 TCR tg mice. (A) Expression of CD3e, CD71, and CD5 on DN subsets (defined as shown in Fig. S4 A). (B) BrdU pulse-labeling experiment. Density plots show intracellular levels of incorporated BrdU in DN thymocytes at different times after a single BrdU injection. (C) Fold change/fold change plot depicting the BDC2.5 tg/non-tg ratio of expression in B697 (x axis) and NOD (y axis) DN4 thymocytes. Blue lines, fold change of 2 (with the number of genes in the corresponding areas). (D) Heat map of 42 cell cycle-related transcripts down-modulated in BDC2.5/B697 DN4 thymocytes (relative expression is color-coded). Cycling (blast) and noncycling (small) DP and γδ thymocytes from ImmGen datasets are included for comparison. (E) Fold change versus mean expression plot depicting B697 versus NOD DN4 thymocyte subsets from BDC2.5 TCR tg (top) and polyclonal mice (bottom). Blue lines, fold change of 1.5. The number of γδ and αβ signature genes above and below this threshold is indicated in green and red, respectively. (F) Proportion of γδ-like CD4⁺CD8[−] DN on gated TCR-β⁺ splenocytes from mice of indicated genotypes. Mean frequencies: 15.4 ± 4.9 (BDC2.5/B697) versus 0.6 ± 0.2 (BDC2.5/NOD); 32.1 ± 11.3 (BDC2.5/B6) versus 3.8 ± 1.5 (BDC2.5/NOD.H2^b). Data are representative of three (A; n ≥ 9 per genotype), eight (B; n ≥ 25 per genotype), two (C–E; n = 2 per genotype per experiment), and three (F; n ≥ 10 per genotype) independent experiments.

In vivo negative selection is functional in NOD mice

Because the previous analyses identified the differential efficiency of the DN to DP transition as the primary cause of the phenotypes observed in TCR tg mice on the NOD background, we reasoned that this same phenomena had likely confused the interpretation of the same models in conditions of in vitro and in vivo negative selection (Lesage et al., 2002; Choisy-Rossi et al., 2004; Zucchelli et al., 2005; Liston et al., 2007; Serreze et al., 2008), putting in jeopardy the arguments that had been used to support a negative selection defect in NOD mice. Therefore, we revisited the efficiency of negative selection in vivo on the

efficiency of the DN to DP transition, resulting in a greater number of DP thymocytes in TCR tg thymi on the NOD background, and thus more intraclonal competition for positive selection niches, ultimately leading to sluggish positive selection.

NOD background, using mixed BM chimera in which niche effects were neutralized. We generated mixed BM chimeras into hosts that expressed a BDC mimotope at low (BDCmi^{LOW}) or high (BDCmi^{HIGH}) levels in thymic epithelial cells, using a

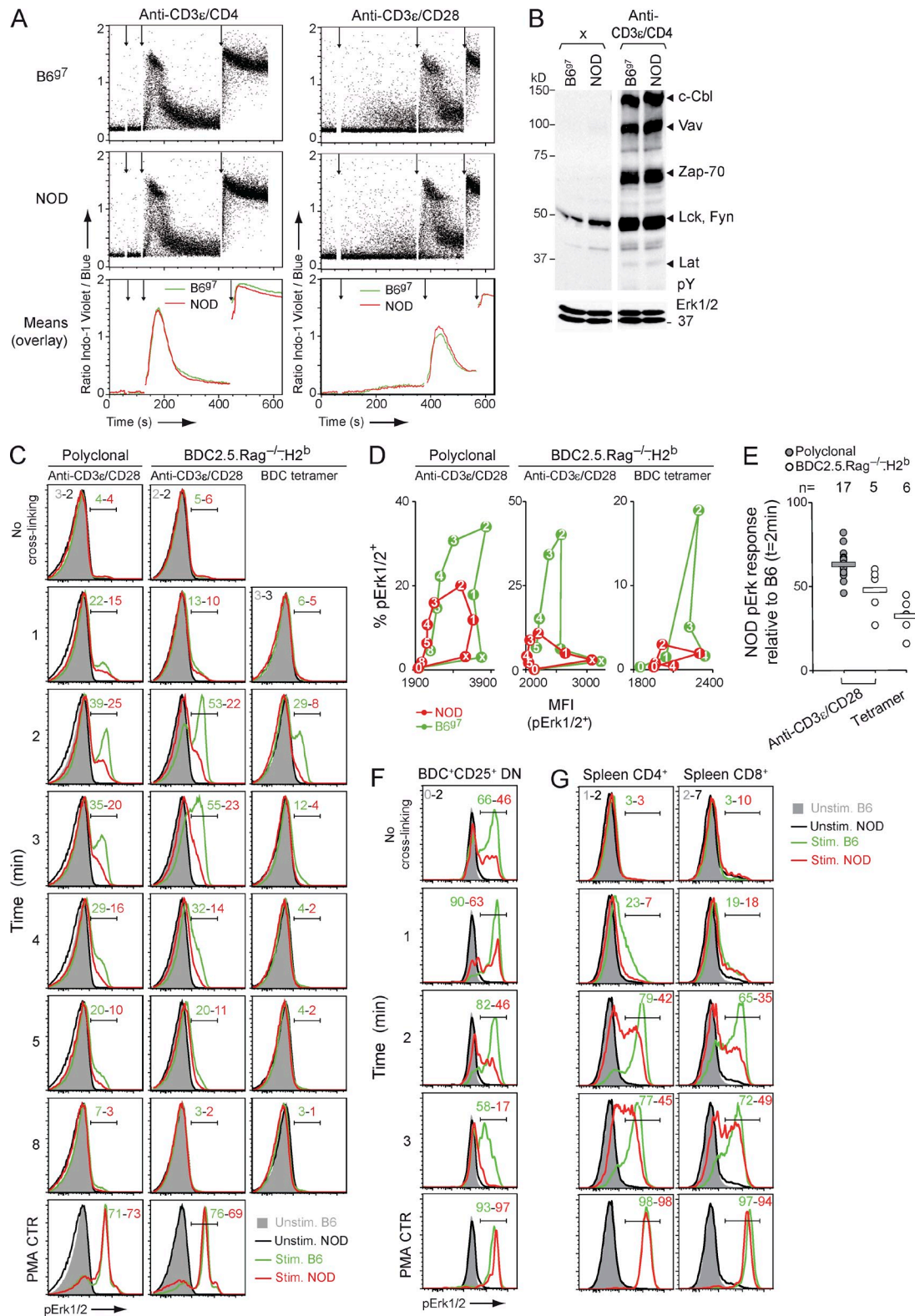


Figure 8. Selective attenuation of Erk1/2 phosphorylation downstream of NOD $\alpha\beta$ -TCRs, rather than global dampening of $\alpha\beta$ -TCR signaling responses. Thymocytes (A–F) or splenocytes (G) were isolated from non-tg B6⁹⁷ and NOD mice or from mice expressing the BDC2.5 tg TCR on a Rag1-deficient, nonselecting B6 and NOD.H2^b backgrounds, mixed in a 1:1 ratio and assessed for TCR-induced signal transduction in the same tube (CD45 congenic markers were used to distinguish B6 and NOD cells after stimulation), except in B where stimulation was performed in separate tubes. (A) Calcium flux induced in polyclonal DP thymocytes by biotinylated primary antibodies (first arrow) and streptavidin cross-linking (second arrow). Third arrow, ionomycin control. Lower panels

tetracycline-regulated expression system (see Materials and methods). BDC2.5/B6 and BDC2.5/NOD BM cells were mixed (polyclonal F1 BM cells were also added to the mix of cells to avoid a massive clonal deletion in the reconstituted thymi) and used to reconstitute F1 control hosts or F1 hosts expressing the BDC2.5 mimotope. As expected, the neo-expression of the BDC2.5 mimotope induced the deletion of a significant number of BDC⁺ thymocytes. On average, the number of BDC⁺ CD4SP was decreased by $55 \pm 16\%$ ($n = 12$) in hosts expressing the mimotope at low dose, whereas the level of deletion further increased to $95 \pm 6\%$ ($n = 10$) for high doses of mimotope expression. Deletion took place mostly at the DP stage (Fig. 6) because both CD4SP and DP subsets were similarly affected by the deletion, whereas DN thymocytes remained mostly unaffected. Importantly, the relative decreases in cell numbers observed in BDC2.5/B6^{g7} and BDC2.5/NOD-derived thymocytes were similar at either dose of mimotope expression (Fig. 6). Thus, negative selection, *in vivo*, is functional on the NOD background.

Tg $\alpha\beta$ -TCRs promote opposite $\gamma\delta$ - and $\alpha\beta$ -lineage fates in B6 and NOD thymocytes

Because the DN to DP transition is driven by the $\alpha\beta$ -TCR in TCR tg thymi (Trop et al., 2000), understanding the cellular and molecular underpinnings of its differential efficacy on B6 and NOD backgrounds would potentially reveal how NOD genetic variation impinges on $\alpha\beta$ -TCR signaling. Therefore, we analyzed the precursor DN pool (Fig. S4 A). TCRs were expressed on the cell surface at the transition between the DN2a and DN2b stages, and at the same levels on the two backgrounds (Fig. 7 A). Expression of the TCR was associated with the up-regulation of CD5 and the proliferation-associated marker CD71 (transferrin receptor). Whereas CD5 up-regulation was stronger on BDC2.5/B6^{g7} DN thymocytes, likely indicative of stronger TCR signals, the expression of CD71 was transient on these cells and largely down-modulated by the time cells reached the DN4 stage. In contrast, a higher degree of cell cycling was observed in the DN4 pool of BDC2.5/NOD mice, as assessed by the persistence of CD71 at this stage (Fig. 7 A) and the higher fraction of DN cells incorporating BrdU in pulse-labeling experiments (Fig. 7 B). Interestingly, although BDC2.5/NOD cells showed a rapid decrease in BrdU levels during the chase

period, presumably as a result of their differentiation into DP cells, levels remained high in BDC2.5/B6^{g7} DN cells, indicating that a significant fraction of them accumulated at the DN stage (Fig. 7 B).

To characterize the transcriptional impact of the early expression of the tg $\alpha\beta$ -TCR at the DN stage on the two backgrounds, we then generated gene expression profiles from BDC2.5 tg and polyclonal DN2-3 and DN4 subsets. According to a fold change/fold change plot displaying the ratio of expression in BDC2.5 tg versus non-tg DN4 thymocytes from B6^{g7} versus NOD mice (Fig. 7 C), the BDC2.5 TCR induced extensive gene expression changes in DN4 thymocytes. Among the genes repressed by the BDC2.5 TCR in DN4 thymocytes from B6^{g7} mice, a Gene Ontology enrichment analysis identified a cluster of 42 cell cycle-related transcripts (Fig. 7 D). These genes were not repressed or were repressed to a much lower extent in BDC2.5/NOD DN4 thymocytes, consistent with the differential degree of proliferation seen in the previous paragraph.

To determine whether these broad transcriptional changes denoted a particular lineage, we used the most induced and repressed genes (603 gene probes, fold change > 3) to define the footprint of the BDC2.5 TCR on DN progenitors, and rank the cell populations analyzed by the Immunological Genome (ImmGen) Consortium (www.immgen.org; 267 populations covering lymphoid and myeloid lineages) according to the level of expression of these genes (Fig. S4 B). Strikingly, 16 of the 20 top ranked populations belonged to the $\gamma\delta$ -lineage. This assignment was confirmed by highlighting $\alpha\beta$ - and $\gamma\delta$ -lineage commitment signatures (defined independently as described in Fig. S4 C) in Fig. 7 C. Most of the up-regulated genes belonged to the $\gamma\delta$ -lineage signature, whereas many of the down-modulated ones belonged to the $\alpha\beta$ commitment signature. These changes were consistent with earlier studies proposing that premature expression of tg $\alpha\beta$ -TCRs in DN thymocytes commits a significant fraction of these progenitors to the $\gamma\delta$ -lineage (Bruno et al., 1996; Terrence et al., 2000). However, the off-diagonal placement, as well as the total number of gene probes up-regulated or down-regulated by the $\alpha\beta$ -TCR on the two backgrounds (at an arbitrary threshold of twofold change, 1,933 versus 333 on B6^{g7} and NOD backgrounds, respectively; Fig. 7 C), indicated that these transcriptional changes were preferentially induced on the B6^{g7} background, and were much more muted on the NOD

display overlaid mean ratios. (B) Purified polyclonal DP thymocytes were left untreated (x) or stimulated (anti-CD3 ϵ /CD4) before isolation of whole-cell lysates and immunoblotting with antibodies specific for phosphotyrosine (pY) and Erk1/2. Arrowheads indicate presumed proteins based on their expected molecular size. (C) Erk1/2 phosphorylation induced in DP thymocytes from polyclonal or BDC2.5 TCR tg mice by anti-CD3 ϵ /CD28 antibodies or peptide-MHC tetramers. Cells were fixed at the times shown at left, after streptavidin or BDC2.5 tetramer addition (no cross-linking controls in the first row were 2 min after addition of primary antibodies alone). Last row, PMA positive control. Numbers indicate percentage of pErk1/2⁺ cells. (D) Representation of data shown in C as the frequency of p-Erk1/2⁺ cells against the mean fluorescence intensity (MFI) of p-Erk1/2⁺ cells. Time points (in min) are indicated in the circles. x, levels observed in absence of cross-linking. (E) Quantification of data shown in C and D, showing the frequency of pErk⁺ NOD thymocytes at the peak of the response ($t = 2$ min) relative to the frequency of B6 responders. Horizontal lines indicate the mean. (F and G) Impaired Erk1/2 phosphorylation at multiple stages of T cell differentiation on the NOD background. Erk1/2 phosphorylation induced in CD25⁺ DN thymocytes from BDC2.5 TCR tg mice (F) and in polyclonal CD4⁺ and CD8⁺ splenocytes (G) by anti-CD3 ϵ /CD28 antibodies, in the same stimulation conditions as in C. Last row, PMA positive control. Numbers indicate percentage of pErk1/2⁺ cells. Data are representative of three (A; $n = 3$ per genotype), two (B; $n = 2$ per genotype), five (C-E; $n = 17$ per genotype for polyclonal stimulations and $n \geq 5$ per genotype for BDC2.5 TCR tg stimulations), three (F; $n = 5$ per genotype), and two (G; $n = 4$ per genotype) independent experiments.

background. This differential magnitude reflected intrinsic properties of B6 and NOD $\alpha\beta$ -TCR signaling networks and not pre-TCR or generic strain-specific differences because they were not observed in polyclonal mice (Fig. 7 E). Accordingly, B6 but not (or to a much lower extent) NOD $\alpha\beta$ -TCR signalosomes induced most of the transcripts found in thymic $\gamma\delta$ T cells, which include the $\gamma\delta$ -lineage transcription factor *Sox13* (Ciofani and Zúñiga-Pflücker, 2010), *S1pr1*, which promotes cellular egress from the thymus, and genes that are strictly expressed in the $\gamma\delta$ branch of thymocytes, like *Etv5*, *Blk*, *Cpa3*, *Il1r1*, *Rbpms*, and *Tox2* (Fig. 7 C and Fig. S4 D).

To determine whether these commitment programs were functional and effectively diverted DN progenitors toward the $\gamma\delta$ -lineage, we directly compared the transcription factors induced by the BDC2.5 TCR in DN4 thymocytes to the ones equipping polyclonal $\gamma\delta$ T cells (Fig. S4 E, top). The BDC2.5 TCR induced the expression of >70% of the transcription factors expressed in $\gamma\delta$ T cells. To identify the molecular events initiating $\gamma\delta$ T cell fate decision downstream of B6 $\alpha\beta$ -TCR signalosomes, we analyzed the DN2–3 thymocyte subsets that corresponded to the earliest stages of expression of the $\alpha\beta$ -TCR (Fig. S4 E, bottom). Of 188 $\gamma\delta$ transcription factors, only 21 were induced by the BDC2.5 TCR, including previously unknown $\gamma\delta$ fate regulators like *Etv5*, *Tox2*, *Rbpms*, and *Sox5*, as well as the already identified *Sox13* and *Id3* factors. In accordance with the extensive array of $\gamma\delta$ transcription factors induced downstream of B6 $\alpha\beta$ -TCR signalosomes, CD4⁺CD8⁺TCR β ⁺ peripheral cells, described earlier as $\gamma\delta$ -like T cells in TCR tg models (Bruno et al., 1996; Terrence et al., 2000), constituted a substantial fraction of the T cell pool in BDC2.5/B6^{g7} mice, and were 10–20 \times more abundant than in NOD mice, both on selecting and nonselecting backgrounds (Fig. 7 F).

Therefore, in addition to promoting the expression of $\gamma\delta$ fate-associated genes, B6 but not NOD $\alpha\beta$ -TCR signalosomes induced a full $\gamma\delta$ maturation program, associated with thymic export and colonization of peripheral lymphoid organs. In contrast, NOD DNs expressed more of the $\alpha\beta$ -lineage genes and the proliferative program characteristic of $\alpha\beta$ -committed DN thymocytes. This differential branching likely explains the much higher efficacy of the DN to DP transition in BDC2.5/NOD mice.

Selective Erk1/2 defect downstream of $\alpha\beta$ -TCRs in NOD T cells

What is the biochemical nature of the signaling differences driving these contrasting cell fates downstream of B6 and NOD $\alpha\beta$ -TCR signalosomes at the DN stage? As $\alpha\beta$ -TCR rather than pre-TCR signaling was affected (Fig. 7 E), we anticipated that the same signaling defects would be present at other stages where the $\alpha\beta$ -TCR is physiologically expressed in normal mice, in particular at the DP stage. In addition, because current models of $\alpha\beta/\gamma\delta$ commitment propose that the differential strength of signals downstream of pre-TCRs and $\gamma\delta$ -TCRs drive these opposite commitments, we quantified signal transduction downstream of B6 and NOD $\alpha\beta$ -TCRs along several known pathways in DP thymocytes.

We first analyzed calcium mobilization, which is dependent on a functional proximal signaling module (Lck–Zap70–Lat–PLC γ –1). Intracellular calcium concentrations reached very similar levels in polyclonal B6^{g7} and NOD DP thymocytes after TCR stimulation (Fig. 8 A). We then quantified global tyrosine phosphorylation events by immunoblotting extracts from TCR-stimulated DP thymocytes. No obvious defects in the patterns of phosphorylated proteins were detected in NOD cells (Fig. 8 B). These two results excluded the hypothesis of a general dampening of NOD TCR signaling pathways as the cause of the opposite $\alpha\beta/\gamma\delta$ commitments observed in TCR tg mice on NOD and B6 backgrounds. We also analyzed the activation of the Erk1/2 MAPK, one of the key pathways known to be differentially required during TCR-dependent checkpoints in thymocyte differentiation (Ciofani and Zúñiga-Pflücker, 2010; Teixeira and Daniels, 2010). The fraction of cells showing Erk phosphorylation (Fig. 8, C and E), as well as the levels of phosphorylation (Fig. 8 D), were much lower on the NOD than on B6^{g7} background for all time-points tested after either anti-TCR antibody stimulation or more physiological antigen-specific stimulation by peptide–MHC tetramers.

Of note, this defect was not only present in DP thymocytes but also at the other stages where the $\alpha\beta$ -TCR was expressed, including in anti-TCR-stimulated BDC⁺ DN2/3 thymocytes (Fig. 8 F), which corresponded to the earliest stages of expression of the $\alpha\beta$ -TCR in BDC2.5 mice (Fig. 7 A), as well as in anti-TCR-stimulated peripheral CD4⁺ and CD8⁺ T cells from non-tg mice (Fig. 8 G). Together, these results pointed to a selective defect in the Erk1/2 signaling module downstream of $\alpha\beta$ -TCRs on the NOD background.

DISCUSSION

Using several TCR tg mouse models to study thymocyte selection on the NOD background, we show that a marked blockade of positive selection of clonotypic T cells occurs in thymi from TCR tg mice on the NOD background, a blockade caused by higher numbers of DP thymocytes competing for positive selection niches. These higher numbers themselves reflect an enhanced DN to DP transition, which in turn results from the quasi-absence of deviation to the $\gamma\delta$ -lineage, usually imparted by early expression of tg TCRs (Fig. 9). These observations held true on nonselecting backgrounds, a result which, by excluding any contribution of MHC-dependent mechanisms, formally invalidates our earlier model according to which increased DP thymocyte numbers in BDC2.5/NOD result from impaired clonal deletion mechanisms (Zucchelli et al., 2005; Holler et al., 2007). Accordingly, using an in vitro clonal deletion model based on isolated, preselected, and monoclonal DP thymocytes on one hand and in vivo negative selection conditions in mixed BM chimera on the other hand, we found that $\alpha\beta$ -TCR complexes equipped with either B6 or NOD signaling networks show very similar signaling potency and commit DP thymocytes to apoptosis with the same efficiency upon encounter of negatively selecting ligands. Thymic negative selection is therefore functional in NOD mice.

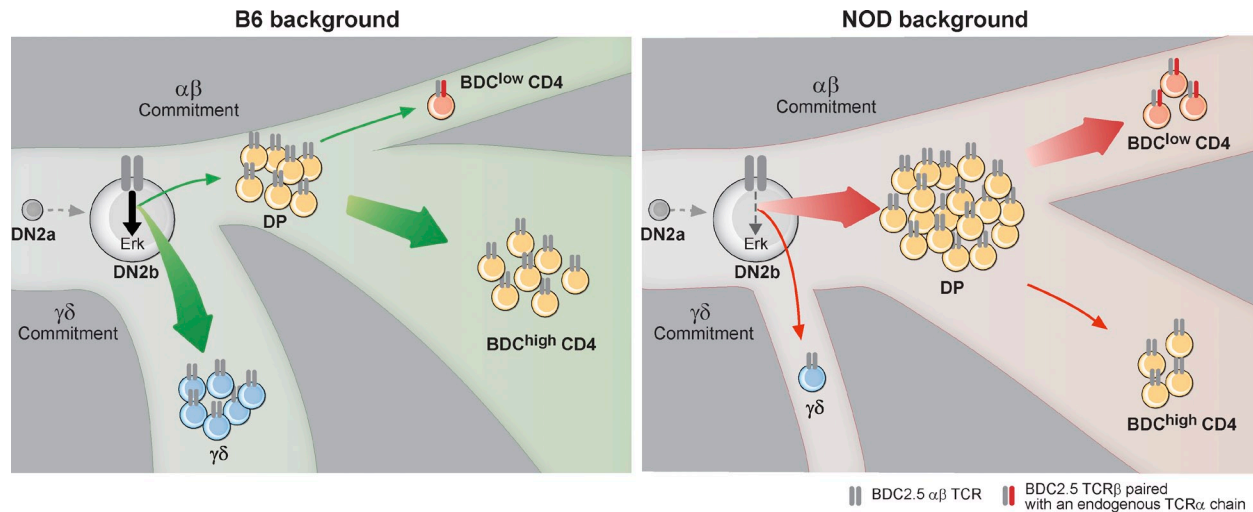


Figure 9. Proposed model, outlining the differential signaling abilities of NOD and B6 $\alpha\beta$ -TCRs to promote $\alpha\beta$ - and $\gamma\delta$ -lineage commitment, when expressed at the DN stage. As a result of the high levels of tg $\alpha\beta$ -TCR expressed on DN thymocytes in TCR tg mice, $\alpha\beta$ -TCRs mimic $\gamma\delta$ -TCRs and divert a significant number of DN progenitors toward the $\gamma\delta$ -lineage on the B6 background (left). Because of a selective defect in the Erk1/2 signaling module, the same tg TCRs wired to NOD signalosomes are perceived like pre-TCRs, rather than $\gamma\delta$ -TCRs, leading to amplification and abundant differentiation into DPs. As a consequence, thymi from NOD TCR tg mice show higher numbers of DP thymocytes than their B6 counterparts, and relatively inefficient positive selection, promoting compensatory rearrangements of endogenous TCR- α loci which rescue some measure of positive selection. This differential decision at the $\alpha\beta/\gamma\delta$ commitment checkpoint explains most of the phenotypes reported in TCR tg NOD mice, among which the impaired selection of TCR tg thymocytes as a result of the saturation of positive selection niches, the higher frequency of receptor editing and clonotype^{low} T cells, and the decreased TCR levels on DP thymocytes. Of note, most T reg cells emerge from the clonotype^{low} fraction in TCR tg models and the higher frequency of clonotype^{low} T cells in BDC2.5/NOD mice results in higher T reg/T conv cell ratios, likely explaining decreased diabetes incidence on this backgrounds.

As purposely emphasized in the Results section, the hallmarks of the divergence at the $\alpha\beta/\gamma\delta$ commitment checkpoint seen in BDC2.5/NOD mice are similarly present in the other TCR tg models for which negative selection defects were reported on the NOD background. It thus seems very likely that, as observed with the BDC2.5 model (and also extended here to the OTII and OTI models), an increased DN to DP transition also leads to the saturation of selection niches in the 3A9 and AI4 systems (indeed, differential DN to DP transition was seen in the mixed BM chimeras of Lesage et al., 2002). Together with a differential efficiency of $\gamma\delta$ deviation (and indeed, much lower proportions of $\gamma\delta$ -like TCR- β^+ DN T cells were recently reported in 3A9 mice on the NOD compared with B10 and BALB/c backgrounds; Dugas et al., 2010), this phenomenon would have obscured an efficient thymic negative selection. Although these predictions await verification, interpretation of the published data in light of our current results strongly suggests that the same mechanisms are at play in these models.

Because of the early TCR expression in TCR tg models and the higher affinity of TCR- α for TCR- β compared with pT α (Trop et al., 2000), $\alpha\beta$ -TCR rather than pre-TCR signalosomes drive the DN to DP transition in TCR tg models. In accordance with earlier hypotheses that tg $\alpha\beta$ -TCRs divert a significant fraction of DN thymocytes toward the $\gamma\delta$ -lineage (Bruno et al., 1996; Terrence et al., 2000; Egawa et al., 2008), transcriptome analyses formally demonstrated that B6 $\alpha\beta$ -TCR signalosomes indeed promote cell-autonomous $\gamma\delta$ commitment

programs of thymic progenitors, early maturation, and thymic egress before the DP stage. Therefore, these cells do not contribute to the DP compartment, explaining the lower DP cellularities and the efficient selection of the BDC2.5 clone seen on the BDC2.5/B6^{g7} background. Of note, this $\gamma\delta$ diversion in TCR tg models was reported on several genetic backgrounds (including B6, B10, and BALB/c; Terrence et al., 2000; Dugas et al., 2010). Therefore, it does not reflect a peculiarity of the B6 background. In contrast, the signaling properties of NOD $\alpha\beta$ -TCR signalosomes stand out as they resemble those of pre-TCR complexes by promoting $\alpha\beta$ rather than $\gamma\delta$ commitment of DN thymocytes (Fig. 9). Contrary to most other TCR tg models on various genetic backgrounds, TCR tg mice on the NOD background therefore show an unusually normal thymic differentiation, with cell numbers and subset frequencies that are much closer to a non-tg thymus.

How to explain then that NOD and B6 $\alpha\beta$ -TCR signalosomes promote equivalent outcomes at the DP stage (cell death by negative selection) but opposite cell fates ($\alpha\beta$ versus $\gamma\delta$ commitment) at the DN stage? Based on the quantitative models of $\alpha\beta/\gamma\delta$ commitment, $\gamma\delta$ commitment requires stronger TCR signals than $\alpha\beta$ commitment and defects in TCR signaling or ligand availability were shown to convert $\gamma\delta$ into $\alpha\beta$ commitment signals (Ciofani and Zúñiga-Pflücker, 2010). However, because quantitative measurements of TCR signaling did not reveal a global dampening or proximal defects in NOD TCR signaling pathways, a generic decrease in TCR signaling strength is not likely to account for the differential $\alpha\beta/\gamma\delta$ commitment

decisions observed in TCR tg models on NOD and B6 backgrounds. In contrast, the selective defect in Erk1/2 activation on the NOD background makes a particularly attractive candidate, as Erk1/2 and the *Id3* levels they control were shown to be crucial regulators of $\alpha\beta/\gamma\delta$ commitment, with the adoption of the $\gamma\delta$ fate being associated with greater Erk1/2 phosphorylation (Hayes and Love, 2002; Haks et al., 2005; Hayes et al., 2005). Because tg $\alpha\beta$ -TCRs are expressed at high levels on DN thymocytes compared with pre-TCR complexes in polyclonal mice, we propose that such high receptor density conveys strong, $\gamma\delta$ -like Erk1/2 signals that instruct $\gamma\delta$ -lineage differentiation on the B6 background. In contrast, on the NOD background, high levels of tg $\alpha\beta$ -TCRs do not elicit such high Erk1/2 signals and behave like pre-TCRs. Of note, a recent study showed that pre-TCR-mediated $\alpha\beta$ commitment is less efficient in NOD than in B6 polyclonal mice (Feng et al., 2011). Because Erk1/2 defects are likely present downstream of NOD pre-TCRs and because pre-TCRs are expressed in limiting amounts on the cell surface of DN thymocytes, contrary to the highly expressed $\alpha\beta$ -TCRs in TCR tg settings, we anticipate that the same defect might hamper (rather than promote) the pre-TCR-driven DN to DP transition in polyclonal settings, a prediction which agrees with the aforementioned study (Feng et al., 2011). Therefore, the results observed here in TCR tg settings are not directly transposable to polyclonal settings, as a result of the very different density of receptors driving the DN to DP transition in TCR tg versus polyclonal settings.

Erk1/2 kinases were shown to be dispensable during thymocyte negative selection (McGargill et al., 2009). Therefore, this selective defect fits well with the observation that clonal deletion and associated transcriptional responses are intact on the NOD background. Similarly illustrating that not all functional outcomes are equally dependent on the Erk1/2 module, the conditional deletion of *Erk2* in peripheral CD8⁺ T cells recently revealed its selective requirement for T cell survival but not for T cell activation or effector functions (D'Souza et al., 2008). The depressed phosphorylation of Erk1/2 is also present in mature NOD T cells. The functional relevancy of this defect in peripheral T cells for T1D will require further investigation, but it is noteworthy that T cell defects in the phosphorylation of Erk1/2 were recently reported in two other autoimmune conditions, in lupus (Gorelik and Richardson, 2010) and rheumatoid arthritis (Singh et al., 2009).

Erk1/2 kinases are required for positive selection of conventional T cells (T conv cells; Fischer et al., 2005) and agonist-selected T reg cells (Willoughby et al., 2007). Surprisingly, however, the reduced Erk1/2 signaling on the NOD background has no discernable effect on the positive selection of thymocytes expressing the fixed BDC2.5 TCR in mixed chimera settings. If anything, selection is actually more efficient on the NOD background. One might speculate that, depending on the affinity of each particular TCR for its positively selecting ligands, such a selective dampening of Erk1/2 responses in NOD thymocytes might favor, impair, or not affect its selection by shifting the Erk1/2 signal inside or outside

the optimal window of selection. Thus, when considering a polyclonal repertoire, one might predict that the affinity threshold for positive selection, and thereby overall affinities of T conv TCRs for self-MHCp, may be higher in NOD mice. Because Erk1/2 kinases are dispensable for effector functions of peripheral T cells (D'Souza et al., 2008), this selective defect would not attenuate the higher reactivity of peripheral T cells, in agreement with the enhanced proliferative T cell responses recently reported in NOD mice (D'Alise et al., 2008). Conceivably, by narrowing the set of self-peptides that would reach the affinity and pERK thresholds required for T reg cell selection, this defect might also explain recent results showing that, despite their apparent normal thymic development, TCR diversity within the NOD T reg cell compartment is markedly restricted (Ferreira et al., 2009). Supporting these hypotheses, the positive selection of invariant NKT (iNKT) cells, which is also Ras-Mapk-Egr dependent (Hu et al., 2011), is impaired in NOD mice that have few thymic iNKT cells (Gombert et al., 1996). Because iNKT cells express an invariant TCR, no repertoire compensation could counterbalance the Erk1/2 defect, potentially explaining their decreased numbers in NOD mice.

In conclusion, the cellular and molecular dissection of thymic selection in NOD mice using multiple TCR tg models yields two key conclusions. First, thymic negative selection does not appear to be at the root of autoreactivity in this model. Second, instead of a global dampening, NOD TCR signaling networks show a selective defect in the Erk1/2 signaling module. We therefore propose the working hypothesis that the emergence of autoreactivity might be favored in NOD mice by a shifted positive selection window and an overall higher reactivity of peripheral T cells for self-MHCp. Although new genetic tools will be required to directly test this model, it constitutes a new lead to the broader question of the mechanisms by which central tolerance failures lead to the emergence of autoreactive T cells in autoimmune diseases.

MATERIALS AND METHODS

Mice. All mice were maintained in specific pathogen-free facilities at Harvard Medical School (Institutional Animal Care and Use Committee, 02954). BDC2.5 TCR tg mice on C57BL/6.H2^b and NOD background were previously described (Katz et al., 1993). BDC2.5/NOD.Rag^{-/-} and BDC2.5/B6^{g7}.Rag^{-/-} mice were derived by crossing the previous lines with NOD.Rag^{-/-} and B6^{g7}.Rag^{-/-} lines, respectively, and diabetes occurrence was prevented by neonatal i.p. injection of total spleen cells from (B6^{g7}xNOD) F1 mice, as described previously (Gonzalez et al., 2001). Similar breeding strategies were used to obtain BDC2.5 TCR tg lines on Rag-sufficient or -deficient B6 and NOD.H2^b background (NOD.H2^b line was previously described; Wicker et al., 1992). TCR- $\alpha^{-/-}$ /NOD, MHC-deficient (IA $\beta^{-/-}$ β 2m^{-/-}), OTII, and OTI.Rag^{-/-} mice were previously described (Philpott et al., 1992; Grusby et al., 1993; Barnden et al., 1998; Clarke et al., 2000). OTII/F1.H2^b and OTI.Rag^{-/-}/F1.H2^b mice were derived by crossing the latter with NOD.H2^b and NOD.H2^b.Rag^{-/-} mice, respectively. For BM chimeras, polyclonal and BDC2.5 TCR tg mice on (B6^{g7}xNOD) F1.H2^{g7} background were generated. NOD mice expressing the BDC mimotope were generated by crossing the tetO-BDCmi mouse line (described in the next section; on the NOD background) with CII-tTA mice (Witherden et al., 2000; expressing the transcriptional activator under the control of the MHC E α promoter, driving the expression in thymic epithelium; backcrossed on

the NOD background for >12 generations). Unless otherwise specified, all mice were analyzed between 4 and 6 wk of age.

Generation of tetO-BDCmi mice. To generate this mouse line encoding a tetracycline (tet)-inducible BDC2.5 mimotope (BDCmi#1, sequence = RTRPLWVRME), the pTiB construct was generated from the pTIM vector, as previously described (van Santen et al., 2004). This vector consists of seven tetO sequences, a CMV minimal promoter, rabbit β -globin intron 2, the mouse class II-associated invariant chain (Ii) peptide region in which amino acids 88–89 have been replaced by an MCC peptide, and the rabbit β -globin 3'-UTR with a poly(A)⁺ RNA site. The pTiB plasmid was constructed via a two-step overlap PCR strategy replacing the MCC peptide with the BDC2.5 mimotope peptide. A PvuI-XhoI fragment derived from pTiB was injected into NOD fertilized eggs and transgene positive founders were selected.

Cell purification and sorting. DN thymocytes were purified by CD4/CD8 complement-mediated depletion, as previously described (Laurent et al., 2004), and subdivided by cell sorting using an ARIA-II (BD). A dump channel was used to exclude CD19, CD11c, CD11b, CD49b, TCR- $\gamma\delta$, and GR1-positive cells. For polyclonal DN populations, CD3 ϵ was included in the dump channel. For clonal deletion assays and biochemistry, DP thymocytes were purified by magnetic CD8 positive selection (Invitrogen; purity >95%). For microarrays, cells were double sorted (purity > 99.9%) directly into Trizol.

Flow cytometry. All fluorochrome-conjugated and biotinylated antibodies were purchased from BD, eBioscience, or BioLegend, except for the biotinylated antibody directed against the BDC2.5 TCR (Kanagawa et al., 2002), which was produced in the laboratory, and for biotinylated I-A^b/BDC2.5 mimotope monomers (AHHPIWARMMA), which were obtained from the National Institutes of Health Tetramer Facility. Cell events were collected using an LSR-II cytometer (BD) and analyzed with FlowJo software (Tree Star).

Microarrays. RNA was prepared from double-sorted cell populations using Trizol, as previously described (Yamagata et al., 2004). RNA was amplified for two rounds (MessageAmp aRNA; Invitrogen), biotin labeled (BioArray High Yield RNA Transcription Labeling; Enzo Life Sciences), and purified with the RNeasy Mini kit (QIAGEN). The resulting cRNAs were hybridized to GeneChip Mouse Genome M1.0 ST chips arrays (Affymetrix). The image reads were processed through Affymetrix software to obtain raw .cel files, background corrected and normalized using the RMA algorithm implemented in the Expression File Creator module from the GenePattern software package (Reich et al., 2006). The cell populations analyzed were generated in duplicate and replicates were averaged. Data were analyzed with the Multiplot module from GenePattern. Microarray data are available from the National Center for Biotechnology Information/GEO repository under accession no. GSE34936.

In vitro clonal deletion assay. Purified DP thymocytes from B6 and NOD background were mixed in a 1:1 ratio and co-cultured for various times with CD3/CD49b-depleted splenocytes from TCR- $\alpha^{-/-}$ /NOD mice (ratio DP/APC of 1:2.5) that were previously pulsed for 2 h with graded concentrations of mimotope peptides (BDCmi#1: RTRPLWVRME [Judkowski et al., 2001]; #2: RTLALWVRME; #3: KVLAVWVRMME) in serum-free medium or were incubated in medium only (for the unstimulated condition). The frequency of remaining viable cells was measured using 0.1 μ g/ml DAPI, Annexin V (according to the manufacturer's instructions; BD), and SSC/FSC plots.

FTOCs. Fetal thymus lobes were dissected from E15.5 embryos. Organs were cultured on sponge-supported filter membranes (Gel Foam surgical sponges, Pharmacia; Supor450 membrane, 0.45- μ m pore size; Pall Gelman Laboratory, VWR) at an interphase between 5% CO₂-humidified air and complete culture medium. Cell suspensions were prepared from FTOC cultures at day 7 by mechanical disruption of the lobes.

BrdU labeling. 1.6 mg BrdU (Sigma-Aldrich) was injected i.p. at the indicated time points before harvest. Thymocytes were fixed, permeabilized, and stained using the APC BrdU flow kit (BD) per the manufacturer's instructions.

BM chimeras. Lethally irradiated host mice (1,000 rad) were injected i.v. with 5×10^6 CD3/CD5/CD49b-depleted BM cells isolated from the femurs of donor mice. Mixed chimeras were performed by mixing BDC2.5/B6 and BDC2.5/NOD donor cells at indicated ratios. For analysis of in vivo clonal deletion, NOD mice carrying the tetO-BDC2.5mi transgene (generated as described in Generation of tetO-BDCmi mice) and the CII-tTA transgene (Witherden et al., 2000) were crossed with B6^{g7} mice to generate (B6^{g7}xNOD) F1 mice carrying either one or the two transgenes. The combination of the two transgenes drove a very strong expression of the BDCmi that resulted in an almost complete deletion of BDC2.5 T cells. Two other settings providing milder expression of the mimotope were therefore established, one that gave very low expression of the mimotope (BDCmi^{LOW}; tetO-BDC2.5 construct in absence of the CII-TA tg, corresponding to a low, TA-independent, leaky expression of the tetO promoter; Lewandowski, 2001) and a second that gave higher expression of the mimotope (BDCmi^{HIGH}; tetO-BDC2.5 construct combined with CII-TA tg, in the presence of 20 μ g/ml doxycycline [Sigma-Aldrich], provided in drinking water for the whole time of the reconstitution). Doxycycline-supplemented water was changed three times per week. Chimeras were analyzed 8 wk after reconstitution.

Calcium flux measurement. B6 and NOD total thymocytes were resuspended in a 1:1 ratio before loading with the calcium indicator Indo-1 (Invitrogen) as previously described (Wang et al., 2005). Baseline Indo-1 fluorescence was recorded at 37°C before the addition of 5 μ g/ml of biotinylated stimulatory antibodies, 10 μ g/ml streptavidin, and 1.4 μ M ionomycin. Calcium responses were analyzed with FlowJo kinetics platform.

Biochemistry. 5.10⁶ DP thymocytes were resuspended in a volume of 100 μ l and stimulated for 2 min at 37°C with 5 μ g of biotinylated anti-CD3, 5 μ g anti-CD4, and 7 μ g avidin. After lysis in TNE buffer (50 mM Tris, 1% Nonidet P-40, and 20mM EDTA) supplemented with protease and phosphatase inhibitors, lysates were subjected to immunoblot analysis. Antibodies against phosphotyrosine and Erk1-2 were purchased from Cell Signaling Technology.

Phospho-flow analysis. B6 and NOD total thymocytes were resuspended in a 1:1 ratio in medium containing 5 μ g/ml of the biotinylated stimulatory antibodies and incubated for 2 min at 37°C before addition of 20 μ g/ml streptavidin. At various times after cross-linking (or addition of 10 μ g/ml I-A^b/BDC2.5 tetramer), cells were fixed, permeabilized, and stained as previously described (Adachi and Davis, 2011). PMA controls were fixed 3 min after addition of 10 ng/ml PMA.

Online supplemental material. Fig. S1 shows the flow cytometry isolation strategy of preselected B6 and NOD DP thymocytes and kinetic microarray analysis of thymic negative selection programs on the two backgrounds. Fig. S2 shows the flow cytometry gating strategy used to identify clonotype^{low} T cells in BDC2.5 TCR tg mice. Fig. S3 shows the flow cytometry gating strategy used to generate the BrdU plot shown in Fig. 2 H. Fig. S4 shows the flow cytometry gating strategy and microarray datasets used to isolate and characterize DN thymocyte subsets in BDC2.5 TCR tg mice. Online supplemental material is available at <http://www.jem.org/cgi/content/full/jem.20112593/DC1>.

We thank D. Burzyn for critical reading of the manuscript, K. Hattori, A. Ortiz-Lopez, and N. Asinowski for mice and antibodies, J. Moore, A. Kressler, J. LaVecchio, G. Buruzala, and V. Toxavidis for flow cytometry, and C. Laplace for assistance with figure preparation. Interpretation of results benefited from data assembled by the ImmGen consortium. The A^b/BDC2.5 tetramer was obtained through the National Institutes of Health Tetramer Facility.

This work was supported by grant 4-2007-1057 from the Juvenile Diabetes Research Foundation. M. Mingueneau was supported by postdoctoral fellowships from the European Molecular Biology Organization (EMBO-ALTF 1087) and the Human Frontier Science Program (HFSP- LT000096).

The authors have no conflicting financial interests.

Submitted: 7 December 2011

Accepted: 17 January 2012

REFERENCES

- Adachi, K., and M.M. Davis. 2011. T-cell receptor ligation induces distinct signaling pathways in naive vs. antigen-experienced T cells. *Proc. Natl. Acad. Sci. USA*. 108:1549–1554. <http://dx.doi.org/10.1073/pnas.1017340108>
- Baldwin, T.A., K.A. Hogquist, and S.C. Jameson. 2004. The fourth way? Harnessing aggressive tendencies in the thymus. *J. Immunol.* 173: 6515–6520.
- Barnden, M.J., J. Allison, W.R. Heath, and F.R. Carbone. 1998. Defective TCR expression in transgenic mice constructed using cDNA-based alpha- and beta-chain genes under the control of heterologous regulatory elements. *Immunol. Cell Biol.* 76:34–40. <http://dx.doi.org/10.1046/j.1440-1711.1998.00709.x>
- Bruno, L., H.J. Fehling, and H. von Boehmer. 1996. The alpha beta T cell receptor can replace the gamma delta receptor in the development of gamma delta lineage cells. *Immunity*. 5:343–352. [http://dx.doi.org/10.1016/S1074-7613\(00\)80260-5](http://dx.doi.org/10.1016/S1074-7613(00)80260-5)
- Buch, T., F. Rieux-Laucat, I. Förster, and K. Rajewsky. 2002. Failure of HY-specific thymocytes to escape negative selection by receptor editing. *Immunity*. 16:707–718. [http://dx.doi.org/10.1016/S1074-7613\(02\)00312-6](http://dx.doi.org/10.1016/S1074-7613(02)00312-6)
- Choisy-Rossi, C.M., T.M. Holl, M.A. Pierce, H.D. Chapman, and D.V. Serreze. 2004. Enhanced pathogenicity of diabetogenic T cells escaping a non-MHC gene-controlled near death experience. *J. Immunol.* 173: 3791–3800.
- Ciofani, M., and J.C. Zúñiga-Pflücker. 2010. Determining $\gamma\delta$ versus $\alpha\beta$ T cell development. *Nat. Rev. Immunol.* 10:657–663.
- Clarke, S.R., M. Barnden, C. Kurts, F.R. Carbone, J.F. Miller, and W.R. Heath. 2000. Characterization of the ovalbumin-specific TCR transgenic line OT-I: MHC elements for positive and negative selection. *Immunol. Cell Biol.* 78:110–117. <http://dx.doi.org/10.1046/j.1440-1711.2000.00889.x>
- D'Alise, A.M., V. Auyeung, M. Feuerer, J. Nishio, J. Fontenot, C. Benoist, and D. Mathis. 2008. The defect in T-cell regulation in NOD mice is an effect on the T-cell effectors. *Proc. Natl. Acad. Sci. USA*. 105:19857–19862. <http://dx.doi.org/10.1073/pnas.0810713105>
- D'Souza, W.N., C.F. Chang, A.M. Fischer, M. Li, and S.M. Hedrick. 2008. The Erk2 MAPK regulates CD8 T cell proliferation and survival. *J. Immunol.* 181:7617–7629.
- Dugas, V., C. Beauchamp, G. Chabot-Roy, E.E. Hillhouse, and S. Lesage. 2010. Implication of the CD47 pathway in autoimmune diabetes. *J. Autoimmun.* 35:23–32. <http://dx.doi.org/10.1016/j.jaut.2010.01.002>
- Egawa, T., T. Kreslavsky, D.R. Littman, and H. von Boehmer. 2008. Lineage diversion of T cell receptor transgenic thymocytes revealed by lineage fate mapping. *PLoS ONE*. 3:e1512. <http://dx.doi.org/10.1371/journal.pone.0001512>
- Feng, N., P. Vegh, E.V. Rothenberg, and M.A. Yui. 2011. Lineage divergence at the first TCR-dependent checkpoint: preferential $\gamma\delta$ and impaired $\alpha\beta$ T cell development in nonobese diabetic mice. *J. Immunol.* 186:826–837. <http://dx.doi.org/10.4049/jimmunol.1002630>
- Ferreira, C., Y. Singh, A.L. Furmanski, F.S. Wong, O.A. Garden, and J. Dyson. 2009. Non-obese diabetic mice select a low-diversity repertoire of natural regulatory T cells. *Proc. Natl. Acad. Sci. USA*. 106:8320–8325. <http://dx.doi.org/10.1073/pnas.0808493106>
- Fischer, A.M., C.D. Katayama, G. Pagès, J. Pouyssegur, and S.M. Hedrick. 2005. The role of erk1 and erk2 in multiple stages of T cell development. *Immunity*. 23:431–443. <http://dx.doi.org/10.1016/j.immuni.2005.08.013>
- Gombert, J.M., A. Herbelin, E. Tancrede-Bohin, M. Dy, C. Carnaud, and J.F. Bach. 1996. Early quantitative and functional deficiency of NK1⁺-like thymocytes in the NOD mouse. *Eur. J. Immunol.* 26:2989–2998. <http://dx.doi.org/10.1002/eji.1830261226>
- Gonzalez, A., I. Andre-Schmutz, C. Carnaud, D. Mathis, and C. Benoist. 2001. Damage control, rather than unresponsiveness, effected by protective DX5⁺ T cells in autoimmune diabetes. *Nat. Immunol.* 2:1117–1125. <http://dx.doi.org/10.1038/ni738>
- Gorelik, G., and B. Richardson. 2010. Key role of ERK pathway signaling in lupus. *Autoimmunity*. 43:17–22. <http://dx.doi.org/10.3109/08916930903374832>
- Grusby, M.J., H. Auchincloss Jr., R. Lee, R.S. Johnson, J.P. Spencer, M. Zijlstra, R. Jaenisch, V.E. Papaioannou, and L.H. Glimcher. 1993. Mice lacking major histocompatibility complex class I and class II molecules. *Proc. Natl. Acad. Sci. USA*. 90:3913–3917. <http://dx.doi.org/10.1073/pnas.90.9.3913>
- Haks, M.C., J.M. Lefebvre, J.P. Lauritsen, M. Carleton, M. Rhodes, T. Miyazaki, D.J. Kappes, and D.L. Wiest. 2005. Attenuation of gammadeltaTCR signaling efficiently diverts thymocytes to the alphabeta lineage. *Immunity*. 22:595–606. <http://dx.doi.org/10.1016/j.immuni.2005.04.003>
- Hayes, S.M., and P.E. Love. 2002. Distinct structure and signaling potential of the gamma delta TCR complex. *Immunity*. 16:827–838. [http://dx.doi.org/10.1016/S1074-7613\(02\)00320-5](http://dx.doi.org/10.1016/S1074-7613(02)00320-5)
- Hayes, S.M., L. Li, and P.E. Love. 2005. TCR signal strength influences alphabeta/gammadelta lineage fate. *Immunity*. 22:583–593. <http://dx.doi.org/10.1016/j.immuni.2005.03.014>
- Holler, P.D., T. Yamagata, W. Jiang, M. Feuerer, C. Benoist, and D. Mathis. 2007. The same genomic region conditions clonal deletion and clonal deviation to the CD8alphaalpha and regulatory T cell lineages in NOD versus C57BL/6 mice. *Proc. Natl. Acad. Sci. USA*. 104:7187–7192. <http://dx.doi.org/10.1073/pnas.0701777104>
- Hu, T., I. Gimferrer, A. Simmons, D. Wiest, and J. Alberola-Ila. 2011. The Ras/MAPK pathway is required for generation of iNKT cells. *PLoS ONE*. 6:e19890. <http://dx.doi.org/10.1371/journal.pone.0019890>
- Huesmann, M., B. Scott, P. Kisielow, and H. von Boehmer. 1991. Kinetics and efficacy of positive selection in the thymus of normal and T cell receptor transgenic mice. *Cell*. 66:533–540. [http://dx.doi.org/10.1016/0092-8674\(81\)90016-7](http://dx.doi.org/10.1016/0092-8674(81)90016-7)
- Judkowski, V., C. Pinilla, K. Schroder, L. Tucker, N. Sarvetnick, and D.B. Wilson. 2001. Identification of MHC class II-restricted peptide ligands, including a glutamic acid decarboxylase 65 sequence, that stimulate diabetogenic T cells from transgenic BDC2.5 nonobese diabetic mice. *J. Immunol.* 166:908–917.
- Kanagawa, O., A. Militech, and B.A. Vaupel. 2002. Regulation of diabetes development by regulatory T cells in pancreatic islet antigen-specific TCR transgenic nonobese diabetic mice. *J. Immunol.* 168:6159–6164.
- Katz, J.D., B. Wang, K. Haskins, C. Benoist, and D. Mathis. 1993. Following a diabetogenic T cell from genesis through pathogenesis. *Cell*. 74:1089–1100. [http://dx.doi.org/10.1016/0092-8674\(93\)90730-E](http://dx.doi.org/10.1016/0092-8674(93)90730-E)
- Kishimoto, H., and J. Sprent. 2001. A defect in central tolerance in NOD mice. *Nat. Immunol.* 2:1025–1031. <http://dx.doi.org/10.1038/ni726>
- Laurent, J., N. Bosco, P.N. Marche, and R. Ceredig. 2004. New insights into the proliferation and differentiation of early mouse thymocytes. *Int. Immunol.* 16:1069–1080. <http://dx.doi.org/10.1093/intimm/16.10.1069>
- Lesage, S., S.B. Hartley, S. Akkaraju, J. Wilson, M. Townsend, and C.C. Goodnow. 2002. Failure to censor forbidden clones of CD4 T cells in autoimmune diabetes. *J. Exp. Med.* 196:1175–1188. <http://dx.doi.org/10.1084/jem.20020735>
- Lewandoski, M. 2001. Conditional control of gene expression in the mouse. *Nat. Rev. Genet.* 2:743–755. <http://dx.doi.org/10.1038/35093537>
- Liston, A., S. Lesage, D.H. Gray, L.A. O'Reilly, A. Strasser, A.M. Fahrner, R.L. Boyd, J. Wilson, A.G. Baxter, E.M. Gallo, et al. 2004. Generalized resistance to thymic deletion in the NOD mouse; a polygenic trait characterized by defective induction of Bim. *Immunity*. 21:817–830.
- Liston, A., K. Hardy, Y. Pittelkow, S.R. Wilson, L.E. Makaroff, A.M. Fahrner, and C.C. Goodnow. 2007. Impairment of organ-specific T cell negative selection by diabetes susceptibility genes: genomic analysis by mRNA profiling. *Genome Biol.* 8:R12. <http://dx.doi.org/10.1186/gb-2007-8-1-r12>
- Mathis, D., and C. Benoist. 2009. Aire. *Annu. Rev. Immunol.* 27:287–312. <http://dx.doi.org/10.1146/annurev.immunol.25.022106.141532>
- McGargill, M.A., I.L. Ch'en, C.D. Katayama, G. Pagès, J. Pouyssegur, and S.M. Hedrick. 2009. Cutting edge: Extracellular signal-related kinase is not required for negative selection of developing T cells. *J. Immunol.* 183:4838–4842. <http://dx.doi.org/10.4049/jimmunol.0902208>
- Philpott, K.L., J.L. Viney, G. Kay, S. Rastan, E.M. Gardiner, S. Chae, A.C. Hayday, and M.J. Owen. 1992. Lymphoid development in mice congenitally lacking T cell receptor α β -expressing cells. *Science*. 256:1448–1452. <http://dx.doi.org/10.1126/science.1604321>
- Pugliese, A., M. Zeller, A. Fernandez Jr., L.J. Zalcberg, R.J. Bartlett, C. Ricordi, M. Pietropaolo, G.S. Eisenbarth, S.T. Bennett, and D.D. Patel. 1997. The insulin gene is transcribed in the human thymus and transcription levels correlated with allelic variation at the INS VNTR-IDD M2

- susceptibility locus for type 1 diabetes. *Nat. Genet.* 15:293–297. <http://dx.doi.org/10.1038/ng0397-293>
- Rapoport, M.J., A.H. Lazarus, A. Jaramillo, E. Speck, and T.L. Delovitch. 1993. Thymic T cell anergy in autoimmune nonobese diabetic mice is mediated by deficient T cell receptor regulation of the pathway of p21ras activation. *J. Exp. Med.* 177:1221–1226. <http://dx.doi.org/10.1084/jem.177.4.1221>
- Rapoport, M.J., A. Mor, P. Vardi, Y. Ramot, O. Levi, and T. Bistrizter. 1999. Defective activation of p21ras in peripheral blood mononuclear cells from patients with insulin dependent diabetes mellitus. *Autoimmunity*. 29:147–154. <http://dx.doi.org/10.3109/08916939908995385>
- Reich, M., T. Liefeld, J. Gould, J. Lerner, P. Tamayo, and J.P. Mesirov. 2006. GenePattern 2.0. *Nat. Genet.* 38:500–501. <http://dx.doi.org/10.1038/ng0506-500>
- Salojin, K., J. Zhang, M. Cameron, B. Gill, G. Arreaza, A. Ochi, and T.L. Delovitch. 1997. Impaired plasma membrane targeting of Grb2-murine son of sevenless (mSOS) complex and differential activation of the Fyn-T cell receptor (TCR)- ζ -Cbl pathway mediate T cell hyporesponsiveness in autoimmune nonobese diabetic mice. *J. Exp. Med.* 186:887–897. <http://dx.doi.org/10.1084/jem.186.6.887>
- Sato, T., K. Hozumi, K. Kishihara, Y. Kametani, C. Sato, Y. Kumagai, T.W. Mak, and S. Habu. 1996. Evidence for down-regulation of highly expressed TCR by CD4 and CD45 on non-selected CD4+CD8+ thymocytes. *Int. Immunol.* 8:1529–1535. <http://dx.doi.org/10.1093/intimm/8.10.1529>
- Serreze, D.V., C.M. Choisy-Rossi, A.E. Grier, T.M. Holl, H.D. Chapman, J.R. Gahagan, M.A. Osborne, W. Zhang, B.L. King, A. Brown, et al. 2008. Through regulation of TCR expression levels, an Idd7 region gene(s) interactively contributes to the impaired thymic deletion of autoreactive diabetogenic CD8+ T cells in nonobese diabetic mice. *J. Immunol.* 180:3250–3259.
- Siggs, O.M., L.E. Makaroff, and A. Liston. 2006. The why and how of thymocyte negative selection. *Curr. Opin. Immunol.* 18:175–183. <http://dx.doi.org/10.1016/j.coi.2006.01.001>
- Singh, K., P. Deshpande, S. Pryshchep, I. Colmegna, V. Liarski, C.M. Weyand, and J.J. Goronzy. 2009. ERK-dependent T cell receptor threshold calibration in rheumatoid arthritis. *J. Immunol.* 183:8258–8267. <http://dx.doi.org/10.4049/jimmunol.0901784>
- Sohn, S.J., J. Thompson, and A. Winoto. 2007. Apoptosis during negative selection of autoreactive thymocytes. *Curr. Opin. Immunol.* 19:510–515. <http://dx.doi.org/10.1016/j.coi.2007.06.001>
- Starr, T.K., S.C. Jameson, and K.A. Hogquist. 2003. Positive and negative selection of T cells. *Annu. Rev. Immunol.* 21:139–176. <http://dx.doi.org/10.1146/annurev.immunol.21.120601.141107>
- Teixeiro, E., and M.A. Daniels. 2010. ERK and cell death: ERK location and T cell selection. *FEBS J.* 277:30–38. <http://dx.doi.org/10.1111/j.1742-4658.2009.07368.x>
- Terrence, K., C.P. Pavlovich, E.O. Matechak, and B.J. Fowlkes. 2000. Premature expression of T cell receptor (TCR) $\alpha\beta$ suppresses TCR $\gamma\delta$ gene rearrangement but permits development of $\gamma\delta$ lineage T cells. *J. Exp. Med.* 192:537–548. <http://dx.doi.org/10.1084/jem.192.4.537>
- Trop, S., M. Rhodes, D.L. Wiest, P. Hugo, and J.C. Zúñiga-Pflücker. 2000. Competitive displacement of pT alpha by TCR-alpha during TCR assembly prevents surface coexpression of pre-TCR and alpha beta TCR. *J. Immunol.* 165:5566–5572.
- van Santen, H.M., C. Benoist, and D. Mathis. 2004. Number of T reg cells that differentiate does not increase upon encounter of agonist ligand on thymic epithelial cells. *J. Exp. Med.* 200:1221–1230. <http://dx.doi.org/10.1084/jem.20041022>
- Villunger, A., V.S. Marsden, and A. Strasser. 2003. Efficient T cell receptor-mediated apoptosis in nonobese diabetic mouse thymocytes. *Nat. Immunol.* 4:717–718, author reply :718. <http://dx.doi.org/10.1038/ni0803-717>
- Wang, Y., O. Horvath, A. Hamm-Baarke, M. Richelme, C. Grégoire, R. Guinamard, V. Horejsi, P. Angelisova, J. Spicka, B. Schraven, et al. 2005. Single and combined deletions of the NTAL/LAB and LAT adaptors minimally affect B-cell development and function. *Mol. Cell. Biol.* 25:4455–4465. <http://dx.doi.org/10.1128/MCB.25.11.4455-4465.2005>
- Wicker, L.S., M.C. Appel, F. Dotta, A. Pressey, B.J. Miller, N.H. DeLarato, P.A. Fischer, R.C. Boltz Jr., and L.B. Peterson. 1992. Autoimmune syndromes in major histocompatibility complex (MHC) congenic strains of nonobese diabetic (NOD) mice. The NOD MHC is dominant for insulinitis and cyclophosphamide-induced diabetes. *J. Exp. Med.* 176:67–77. <http://dx.doi.org/10.1084/jem.176.1.67>
- Willoughby, J.E., P.S. Costello, R.H. Nicolas, N.J. Robinson, G. Stamp, F. Powrie, and R. Treisman. 2007. Raf signaling but not the ERK effector SAP-1 is required for regulatory T cell development. *J. Immunol.* 179:6836–6844.
- Witherden, D., N. van Oers, C. Waltzinger, A. Weiss, C. Benoist, and D. Mathis. 2000. Tetracycline-controllable selection of CD4+ T cells: half-life and survival signals in the absence of major histocompatibility complex class II molecules. *J. Exp. Med.* 191:355–364. <http://dx.doi.org/10.1084/jem.191.2.355>
- Yamagata, T., D. Mathis, and C. Benoist. 2004. Self-reactivity in thymic double-positive cells commits cells to a CD8 alpha alpha lineage with characteristics of innate immune cells. *Nat. Immunol.* 5:597–605. <http://dx.doi.org/10.1038/ni1070>
- Zhang, J., K. Salojin, and T.L. Delovitch. 1998. Sequestration of CD4-associated Lck from the TCR complex may elicit T cell hyporesponsiveness in nonobese diabetic mice. *J. Immunol.* 160:1148–1157.
- Zucchelli, S., P. Holler, T. Yamagata, M. Roy, C. Benoist, and D. Mathis. 2005. Defective central tolerance induction in NOD mice: genomics and genetics. *Immunity*. 22:385–396. <http://dx.doi.org/10.1016/j.immuni.2005.01.015>

SUPPLEMENTAL MATERIAL

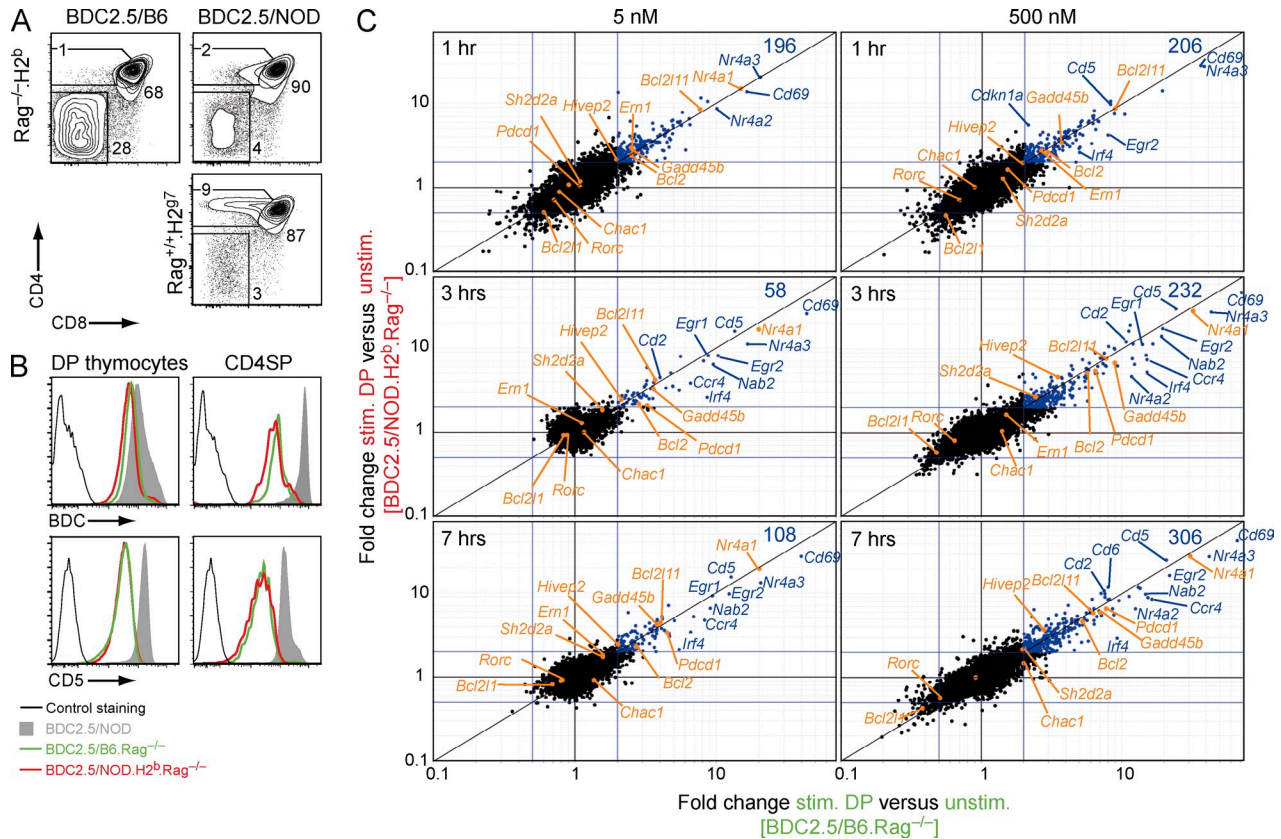
Mingueneau et al. <http://www.jem.org/cgi/content/full/jem.20112593/DC1>

Figure S1. Flow cytometry isolation strategy of preselected B6 and NOD thymocytes and kinetic microarray analysis of negative selection programs on the two backgrounds. (A and B) Characterization of thymocyte subsets from BDC2.5 TCR tg mice expressing the nonselecting H2^b MHC haplotype. Expression of CD4 and CD8 (A) and BDC TCR and CD5 (B) on thymocytes from mice of indicated genotypes. Thin lines indicate control staining. Mean thymic cellularities: 69 ± 20, n = 9 (BDC2.5/B6.Rag^{-/-}); 153 ± 41, n = 8 (BDC2.5/NOD.H2^b.Rag^{-/-}). (C) Pre-selected DP thymocytes were purified and stimulated as described in Fig. 1. Fold change/fold change plots depict the stimulated (stim.)/unstimulated (unstim.) ratio of expression in B6 (x axis) and NOD (y axis) DP thymocytes at 1, 3, and 7 h after stimulation with 5 nM (left) or 500 nM (right) BDC mimotope (BDCmi#1). Blue lines, fold change of 2. Genes induced more than two times in B6 and NOD thymocytes are highlighted in blue with the corresponding number of induced genes in the upper right corner of each plot. Genes that were previously associated with thymic negative selection are indicated in orange. Data are representative of three (A and B; n ≥ 8 per genotype) and means of two (C; n = 2 per genotype for t = 1 and 3 h and n = 4 per genotype for t = 7 h) independent experiments.

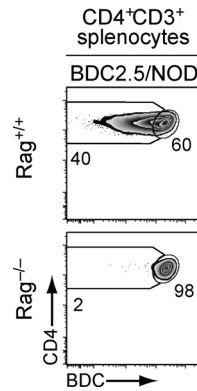


Figure S2. Flow cytometry gating strategy used to identify clonotype^{low} T cells in BDC2.5 mice. Splenocytes were isolated from mice expressing the BDC2.5 Tg TCR on a *Rag1*-proficient (*Rag*^{+/+}) or -deficient (*Rag*^{-/-}) NOD background. Expression of CD4 and BDC TCR on CD4⁺CD3⁺ splenocytes. Numbers in outlined areas indicate percentage of BDC^{high} and BDC^{low} cells. Data are representative of two independent experiments ($n \geq 4$ per genotype).

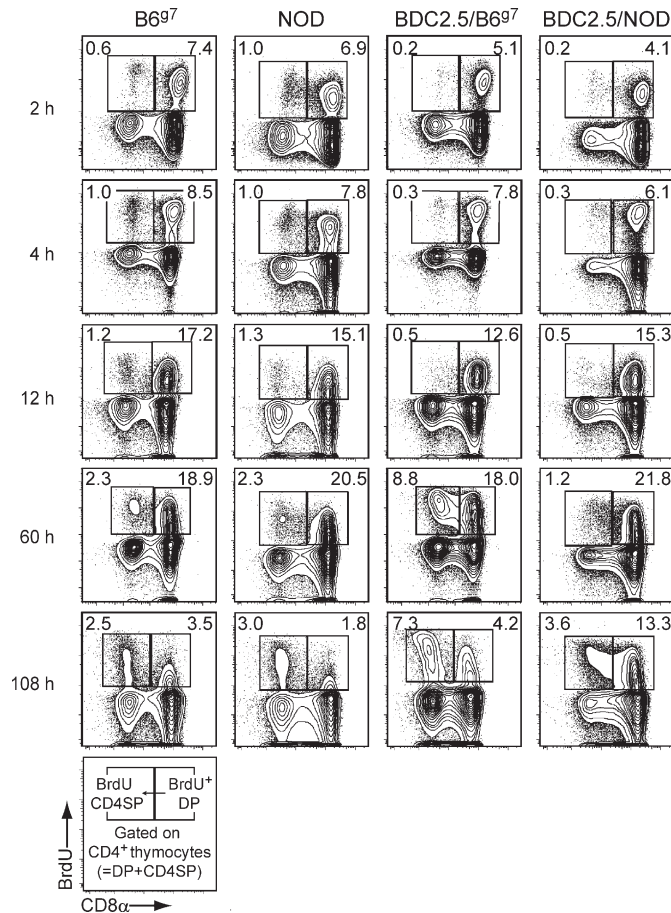


Figure S3. Flow cytometry gating strategy used to generate BrdU data shown in Fig. 2 H. Kinetics of BrdU⁺ thymocyte differentiation in polyclonal and BDC2.5 TCR tg mice at indicated time points (left margin) after a single BrdU injection. Density plots (used to generate Fig. 2 H) show intracellular levels of incorporated BrdU and expression of CD8 on CD4⁺-gated thymocytes (see gating scheme). Data are representative of eight independent experiments ($n \geq 17$ per genotype for polyclonal mice and $n \geq 25$ per genotype for BDC2.5 TCR tg mice).

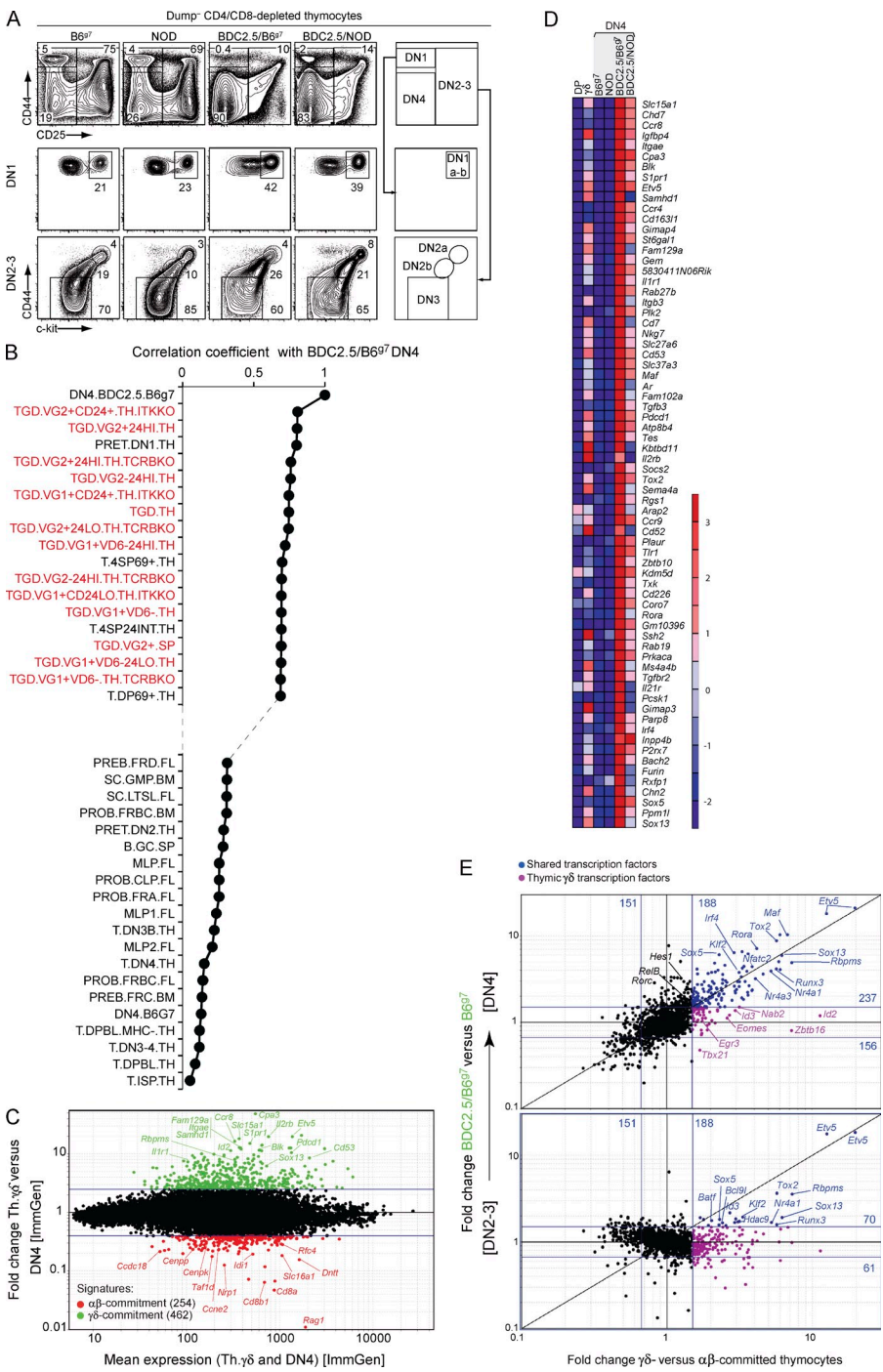


Figure S4. Flow cytometry gating strategy and microarray datasets used to isolate and characterize DN thymocyte subsets in BDC2.5 TCR tg mice. Thymocytes were isolated from polyclonal or BDC2.5 TCR tg mice on B6g7 or NOD background. After CD4 and CD8 complement-mediated depletion, CD4⁺CD8⁺ DN thymocytes were analyzed by flow cytometry (A) or microarray (B–E). (A) Purification and gating strategy used to identify DN thymocyte subsets in TCR tg mice. Expression of CD44 and CD25 on DN thymocytes (top) and CD44 and CD117 (c-kit) on DN1 (middle) and DN2–3 (bottom) thymocyte subsets from mice of indicated genotypes. (B) DN4 thymocytes from polyclonal and BDC2.5 TCR tg mice were isolated and analyzed by transcriptome profiling. Ranking of the populations from the ImmGen Consortium dataset (267 populations) according to the level of expression of the signature genes defining the transcriptional footprint of the BDC2.5 TCR on DN4 thymocytes (these signature genes were defined as showing fold change expression values [DN4 BDC2.5/B6g7 vs. DN4 B6g7] >3 or <0.3). Pearson's correlation coefficients were calculated for each ImmGen population relative to the DN4 subset from BDC2.5/B6g7 mice, based on the expression values of the 603 genes from the signature. The 20 populations showing the highest (top) and lowest (bottom) correlation values are displayed. Populations from the γδ-lineage are displayed in red. (C) Definition of αβ and γδ commitment signatures. Fold change versus mean expression plot depicting thymic (Th) γδ versus DN4 subsets (from the ImmGen Consortium dataset). αβ (red) and γδ commitment (green) signature genes were defined as the genes expressed >2.5× (blue lines) in DN4 versus Th.γδ and vice versa, respectively. (D) Heat map of the most induced transcripts in DN4 thymocytes by the BDC2.5 tg TCR (genes were defined as showing fold change expression values [DN4 BDC2.5/B6g7 vs. DN4 B6g7] >6). Genes are ranked by decreasing inducibility from top to bottom, and for each gene expression is color-coded according to its relative value (see key). For comparison, gene expression values in DP and γδ thymocytes from the ImmGen Consortium dataset are included. (E) Fold change/fold change plot depicting the expression ratio from γδ- versus αβ-committed thymocytes (ratio of thymic γδ vs. DN4, ImmGen dataset, x axis) versus the BDC2.5 tg/non-tg ratio of expression in DN4 (top) and DN2–3 thymocytes (bottom) from B6g7 mice (y axis). Data are filtered on a list of 1,680 known or putative transcription factors. Data are representative of two (A; n ≥ 2 per genotype for polyclonal mice and n ≥ 9 per genotype for BDC2.5 TCR tg mice) and two (B–E; n = 2 per genotype per experiment) independent experiments.

Downloaded from jem.rupress.org on February 17, 2012